



Multidisciplinary study of Holocene archaeological soils in an upland Mediterranean site: Natural versus anthropogenic environmental changes at Cecita Lake, Calabria, Italy



Teresa Pelle^{a,*}, Fabio Scarciglia^a, Gaetano Di Pasquale^b, Emilia Allevato^b,
Domenico Marino^c, Gaetano Robustelli^a, Mauro F. La Russa^a, Iolanda Pulice^a

^a Dipartimento di Biologia, Ecologia e Scienze della Terra (DiBEST), Università della Calabria, Via Pietro Bucci – Cubo 15B, 87036 Arcavacata di Rende, CS, Italy

^b Laboratorio di Storia della Vegetazione e Anatomia del Legno, Università di Napoli "Federico II", Dipartimento di Arboricoltura, Botanica e Patologia Vegetale, Via Università 100, 80055 Portici, NA, Italy

^c Soprintendenza per i Beni Archeologici della Calabria, Ufficio Territoriale di Crotona e della Sila, Via Risorgimento 121, 88900 Crotona, Italy

ARTICLE INFO

Article history:

Available online 10 April 2013

ABSTRACT

This paper highlights results of a multidisciplinary and multi-analytical study of Holocene archaeological soils around Cecita Lake (Sila massif, Calabria, southern Italy), which represents a typical upland Mediterranean environment. It is focused on assessment of climatic and environmental changes that took place since late Neolithic to Roman times, trying to discriminate natural from anthropogenic signals. Based on an integration of archaeological, geomorphological, stratigraphic, pedological, volcanological and soil charcoal (pedoanthracological) data, the following paleoclimatic/environmental reconstruction is proposed: a warm and humid, seasonally contrasted climate, with an overall geomorphological stability suited for soil development, characterized the late prehistoric environment (Holocene climatic optimum), dominated by a widespread oak forest. The main pedogenetic processes consisted in organic matter accumulation, clay illuviation, phyllosilicate and short-range order mineral neogenesis from weathering of granite and volcanic ash, sourced from late Pleistocene–Holocene eruptions of the Aeolian Islands. One or more mid-Holocene episodes of climate deterioration towards drier conditions (indicated by a decrease of clay translocation processes and possible irreversible dehydration of poorly-crystalline aluminosilicates into phyllosilicate clay minerals) promoted intense land degradation. This was in turn enhanced by increasing human activities for settlement and resource exploitation (among which deforestation and ploughing for agriculture), which led to a shift of the vegetation cover towards a dominant pine forest between 3 ka BP and the Roman epoch. Humid and possibly cooler climatic conditions during the late Holocene are indicated by the decrease of clay illuviation, coupled with short-range order components prevailing over phyllosilicate clays during Roman soil formation.

© 2013 Elsevier Ltd and INQUA.

1. Introduction

Impact of Quaternary climate changes on the environment and ancient societies is a matter of discussion in both palaeoclimate and archaeology communities (e.g. Butzer, 2005; Madella and Fuller, 2006; Jalut et al., 2009; Roberts et al., 2011). It was demonstrated by various authors (Anderson et al., 2007; Turney and Brown, 2007; Warner et al., 2010; Mercuri et al., 2011) that climate can have modified human habits since the past and caused civilizations to adapt to climatic changes.

The study of climate oscillations during the Holocene is particularly important because they are in direct temporal continuity with modern climatic conditions. Moreover, Holocene paleoenvironmental research provides a unique way to reconstruct and understand how ecosystems respond to climate changes at longer timescales than short-term bio-geosphere dynamics directly observed, monitored and often quantified by instrumental methods in very recent and present times (cf. Overpeck et al., 2003). In particular, a crucial question exists about role of natural and anthropogenic forcing, which also underlines the need for reliable prediction of forthcoming scenarios, mainly in terms of possible cultural adaptations and responses of modern societies to future climate change (deMenocal, 2001; Gregory et al., 2006). Use of other continental proxies, such as soils and charcoals as indicators

* Corresponding author.

E-mail addresses: teresa.pelle@unical.it, teresa_geo82@yahoo.it (T. Pelle).

of ecosystem responses to Holocene climatic and environmental changes in the Mediterranean, is still less explored (e.g. Sadori et al., 2008; Favilli et al., 2010; Linstädter and Zielhofer, 2010; Vanniere et al., 2011).

The aim of the present work is to investigate the role of soils and soil charcoal as complementary tools to traditional high-resolution continental archives, for assessing the main environmental changes that took place during the Holocene in an upland Mediterranean area of southern Italy, namely Cecita Lake (Sila massif, Calabria region) (Fig. 1a and b). This site has already been shown to have an interesting record of late Quaternary paleoclimatic/environmental changes, weathering and pedogenetic processes, as well as long-term geomorphological evolution (e.g. Scarciglia et al., 2005a,b; 2008). It is therefore a potentially good indicator of the regional environment and still appears as a promising area for further detailed investigations of the Holocene record in soils developed in archaeological contexts. For this purpose we applied a multidisciplinary, geomorphological, stratigraphic, pedological, volcanological paleobotanical and archaeological approach, focusing on characterization of some archaeological sites in the area around Cecita Lake, which span from late Neolithic (3800–3600 BC) to the late Empire Roman Age (5th century AD).

Very few papers have so far dealt with soil charcoal analysis (pedoanthracology) coupled with soil characterization, mainly focused on soil morphological description and/or soil chemistry and organic matter properties (Di Pasquale et al., 2008; Favilli et al., 2010; Egli et al., 2012). Here an innovative integration of soil study, including detailed chemical, physical, mineralogical and micro-morphological analyses, with pedoanthracology was achieved, up to now not applied in the literature: geomorphic evolution and terrestrial ecosystem response to changing climatic conditions are interpreted on the basis of traditional pedological analyses, whereas diachronic vegetation reconstruction, i.e. evaluation of past vegetation dynamics through time, is provided by soil charcoal analysis (Carcaillet and Thinon, 1996; Figueiral and Mosbrugger, 2000; Touflan and Talon, 2009). Both approaches, coupled with other geoarchaeological indicators (traces of agricultural practices, exploitation of raw materials, manufacturing, etc.), are also used in a challenging attempt to discriminate climatic (natural) from non-climatic (anthropogenic) signals. In a region as the circum-Mediterranean basin, characterized by a long and variegated history of human occupation, this effort can be problematic, especially

during the mid to late Holocene transition (e.g. Roberts et al., 2004; Migowski et al., 2006; Thorndycraft and Benito, 2006). In this context, also some peculiar features typical of soils developed on volcanic products, such as clay mineralogy and andic properties (sensu IUSS Working Group WRB, 2007; Soil Survey Staff, 2010) are used as (paleo-) environmental/climatic proxies (e.g. Duchaufour, 1982; Buol et al., 1989; Shoji et al., 1993; Frezzotti and Narcisi, 1996; James et al., 2000).

2. Geological, geomorphological, climatic and vegetation setting

The Sila massif consists of a Paleozoic, high- to low-grade metamorphic basement (gneiss, amphibolite, schist and phyllite) of the Calabrian Peloritani Arc (Amodio-Morelli et al., 1976; Van Dijk et al., 2000), intruded by a late Hercynian Sila batholith (Messina et al., 1991; Caggianelli et al., 2000; Liotta et al., 2008), and in places covered by Mesozoic and Miocene to Pleistocene sedimentary deposits (Roda, 1964; Critelli, 1999; Van Dijk et al., 2000). The Sila batholith consists of different, mutually intersecting plutonic rock intrusions (granodiorite, gabbro and leucomonzogranite).

The landscape of the Sila massif is characterized by gently rolling, dissected limbs of relict planation landforms (paleosurfaces) of Pliocene–Pleistocene ages, with a chessboard-like spatial pattern, cut across the crystalline basement rocks and the sedimentary cover (e.g. Sorriso-Valvo, 1993; Molin et al., 2004; Scarciglia et al., 2005a, 2005b, 2007). These landforms were displaced by tectonic uplift above the present base-level at elevation ranges of 800–1700 m a.s.l. and are bordered by steep slopes with generally high local relief. Some intramontane tectonic depressions characterize the Sila uplands, where large, present-day artificially dammed lakes replace Pleistocene paleo-lakes. The study sites are located along perimetral terraced shores of one of these basins, namely Cecita Lake. A mid to late Pleistocene fluvio-lacustrine sedimentary succession (not less than 15 m thick) represents the paleo-Cecita basin-fill. It consists of yellowish/greenish to light grey/bluish lacustrine clays, alternated with silt, sand and fine gravel beds and dark brown to blackish peaty layers (e.g. Sorriso-Valvo, 1993; Scarciglia et al., 2005a,b). Three orders of terraces of middle to late Pleistocene–Holocene ages are carved on it (Scarciglia et al., 2005b) (Fig. 1b): the higher terrace crops out along the Cecita Valley (to the east of the lake) at about 1270 m a.s.l., where sands, silts, clays and

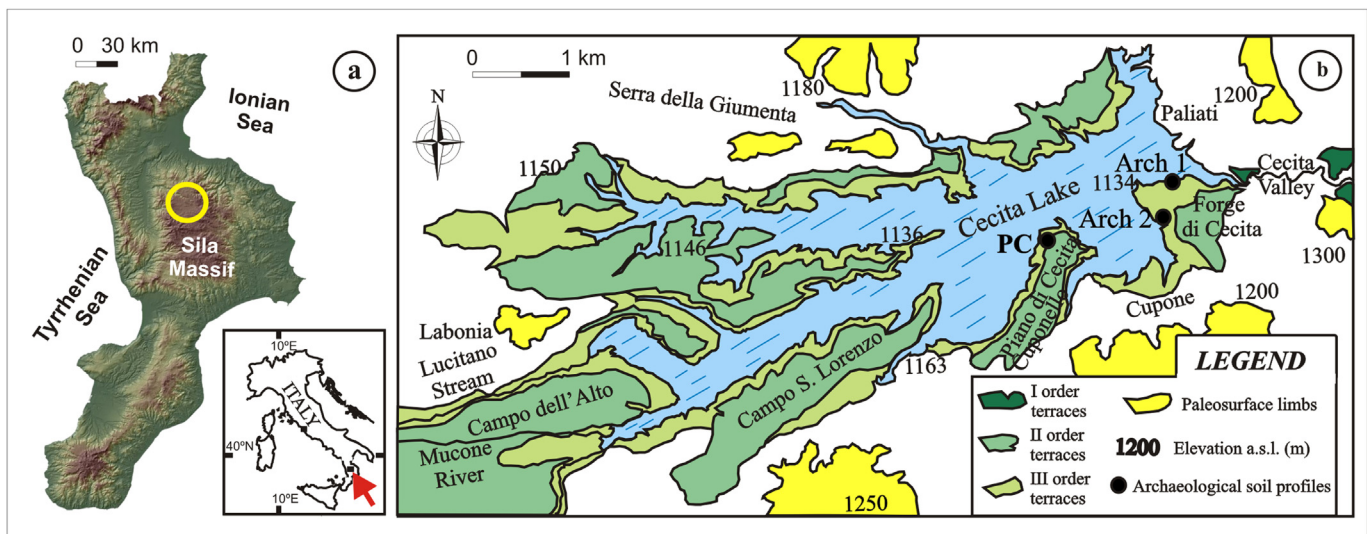


Fig. 1. Location of the study area (a) and geomorphological sketch map of Cecita Lake with the studied archaeological soil profiles (b). Modified from Scarciglia et al. (2005b, 2008).

minor gravels alternate. The intermediate and lower terraces, reaching about 1138–1150 and 1127 m a.s.l. respectively, are morphologically entrenched within these older terraced deposits. In particular, the former developed on gravelly and sandy alluvial sediments that overlie the lacustrine silty and clayey facies, across which the latter are cut.

A widespread soil type, developed on both fluvio-lacustrine deposits and plutonic bedrock, with a contribution of late Pleistocene to Holocene fine volcanic ash during soil formation and consequent weak andic properties (sensu IUSS Working Group WRB, 2007; Soil Survey Staff, 2010), characterizes with lateral continuity all the area around Cecita Lake (ARSSA, 2003; Scarciglia et al., 2005a,b; 2008). It represents a geosol, i.e. a pedostratigraphic marker in the Sila uplands (Scarciglia et al., 2008), which also includes the archaeological soil profiles of late Neolithic/early Eneolithic and Roman ages studied in the present paper. It is commonly exposed at surface, but in places it is buried by detrital slope deposits, where its latest phases of pedogenesis are dated to 3136 ± 19 BP (conventional AMS radiocarbon dating) on the basis of soil charcoal therein included (Scarciglia et al., 2008).

The study area is characterized by a typical upland Mediterranean climate (Csb-type, sensu Köppen, 1936), i.e. a temperate humid climate without a particularly prolonged dry summer. Mean annual precipitation is spread throughout the fall-winter season (with maxima during December and/or January) and reaches about 1500 mm/year, including snowfall. Mean annual temperature is around 8–9 °C, with mean monthly values of –1 °C in the coldest month (January) and of 12–16 °C in the warmest one (August) (Versace et al., 1989; Colacino et al., 1997; ARSSA, 2003). From a pedoclimatic point of view (cf. Soil Survey Staff, 2010) the soils of the Sila uplands are characterized by a mesic temperature regime coupled with an udic moisture regime (ARSSA, 2003).

The vegetation cover is dominated by grassland used for grazing and cultivated fields (mainly wheat and potatoes), beech (*Fagus sylvatica*) and oak forest (*Quercus cerris*) and especially high mountain belt conifers where pine (*Pinus nigra* subsp. *laricio*) prevails and fir (*Abies alba*) occurs subordinately. Most of pines are the result of recent reforestation policies promoted during the last half century (Costantini, 1993), coupled with progressive renaturalization, after repeated phases of intense forest clearance and crop activities until the 1950s (Sorriso-Valvo, 1993).

3. Methods

3.1. Soil analyses

Soil samples from three representative soil profiles of the two archaeological settlements (profile PC, late Neolithic to early Eneolithic; profiles Arch 1 and Arch 2, Roman epoch) (Fig. 1b) were described in the field and sampled for different laboratory analyses. In particular, archaeological findings were used to fix time constraints for the studied soils, in addition to other chronological data already available in the literature (Scarciglia et al., 2005a, 2005b, 2008). Physical and chemical analyses were carried out on soil bulk samples (fine earth fraction, <2 mm) after air-drying and sieving, according to standard procedures (MiPAF, 2000): particle size distribution, pH(NaF) (Fieldes and Perrott, 1966) and pH(H₂O), organic carbon, total carbonate, cation exchange capacity (CEC) and exchangeable bases were determined.

Clay minerals were identified by X-ray diffraction analysis (XRD) on air-dried, parallel-oriented specimens (Hughes et al., 1994) of the clay fraction (<2 μm), using a Rigaku D/MAX-2200/PC instrument (Cu–K α radiation, 40 kW, 30 mA). The following treatments were performed: Mg saturation, ethylene-glycol (EG) solvation, heating at 105 °C, 350 °C and 550 °C (Wilson, 1987; Moore and

Reynolds, 1997). The same samples were analyzed as powders by Fourier transform infrared spectroscopy (FT-IR) using a Nicolet 380 instrument, equipped with a Smart Orbit accessory, operating in ATR (attenuated total reflectance) mode. Absorbance spectra were measured in the mid-infrared region (wavenumbers 400–4000 cm^{–1}).

Different forms of Al, Fe and/or Si were determined on the fine earth fraction (<2 mm) using selective extraction techniques, such as acid ammonium oxalate extractable Al_o, Fe_o, Si_o (Schwertmann, 1964) and sodium pyrophosphate extractable Al_p (Bascomb, 1968). Their amounts were measured by atomic absorption spectroscopy (AAS). On the basis of these extractions, some indices for the estimation of short-range order minerals (SROM), such as allophane, proto-imogolite, imogolite and ferrihydrite, were calculated: Al_o% + 0.5 Fe_o% (ICOMAND, 1988); (Al_o – Al_p)/Si_o and Al_p/Al_o (Parfitt and Wilson, 1985). In particular, the ICOMAND index proposed by the International Committee on the Classification of Andisols was used as a proxy for the assessment of andic properties (IUSS Working Group WRB, 2007; Soil Survey Staff, 2010). This index is based on the fact that oxalate extraction procedures can separate aluminium and iron forms occurring in amorphous (and poorly-crystalline) soil materials, i.e. entering metal–humus complexes and/or short-range order neoformed aluminosilicates. Pyrophosphate extracted aluminium subtracted from oxalate extracted aluminium corrects for removal of Al–humus complexes, thus estimating active Al content incorporated just into allophanic components (Dahlgren et al., 1993; García-Rodeja et al., 2007). Allophane content was calculated using the formula published by Mizota and van Reeuwijk (1989), whereas approximate ferrihydrite content was estimated as proposed by Childs et al. (1990).

Micromorphological observations were performed on thin sections (10 cm × 5 cm × 30 μm) from each genetic horizon of soil profiles Arch 1, Arch 2 and PC, and from an additional buried horizon (Ab) in another late Neolithic to early Eneolithic soil profile (see following section on field features). Thin sections were prepared from undisturbed soil samples, after impregnation with a polyester cristic resin and air-hardening, and described in optical microscopy according to FitzPatrick (1984).

Scanning electron microscopy analyses, coupled with energy dispersive spectroscopy (SEM–EDS), were carried out on the same thin sections to assess possible volcanic components and characterize their chemical composition. A Stereoscan 360 scanning electron microscope (Cambridge Instruments), equipped with a Si/Li-SUTWdetector (EDAX, Philips Electronics), was used.

3.2. Charcoal analysis

The pedological study was complemented by soil charcoal analysis, as a reliable proxy for reconstructing the local woody vegetation with high spatial detail (Carcaillet and Thion, 1996; Touflan et al., 2010).

Analyzed charcoals come from four pedological horizons belonging to the Roman soil profiles (Ap and A from soil profile Arch 1 and A from profile Arch 2) and to the late Neolithic/early Eneolithic one (A, profile PC), as well as from the corresponding archaeological pedofacies extensively exposed in the excavations. Following Carcaillet and Thion (1996), soil samples were taken through the pedological horizons and sieved by water through a sieving column with 2 and 0.4 mm mesh size. All charcoal fragments were dried and sorted under a dissecting microscope to be botanically identified. Taxonomical determinations were made using an incident light microscope at magnification of 100×, 200×, 500× and 1000×, and after comparison with specialist literature, wood anatomy atlases (e.g. Greguss, 1955, 1959; Schweingruber, 1990) and the reference collection of the Laboratory of Vegetation

History and Wood Anatomy (Università di Napoli Federico II, Portici, Italy).

4. Results

4.1. Archaeology

Evidence of human occupation along Cecita Lake shores spans from about 5.8 to 1.5 ka BP. In particular, remains of late Neolithic (3800–3600 BC) to early Eneolithic (3600–3350 BC), Greek (6th to 3rd century BC) and Roman Republican to late Imperial ages (3rd – 1st centuries BC to 5th century AD, respectively) were found during excavations carried out by the Soprintendenza per i Beni Archeologici della Calabria (Superintendence of Archaeological Heritage of Calabria). Several prehistoric/protohistoric settlements were excavated on different limbs of the fluvio-lacustrine terraces along

the southern and eastern margins of the lake, such as Piano di Cecita-Cuponello (Fig. 2a and b), Campo S. Lorenzo, Forge di Cecita and Paliati. They mainly consist of pole holes left by wooden huts and plenty of lithic artefacts, including bowtie-shaped granite weights for hand-throwing fishing nets (Fig. 2c), and flint or obsidian tools and weapons. Pottery vases of the same period were found (Fig. 2d). Well-preserved plough marks with a reticulate pattern of crossing furrows and ridges were identified at Paliati site. On the terrace located at Forge di Cecita, a Greek sanctuary was excavated. In the same area and at Campo S. Lorenzo site Roman colonization is testified by settlements occupied since Republican to late Empire age (Fig. 2e). Among the main findings a complex kiln for pitch extraction and production is noteworthy (Fig. 2f). A number of coins of different provenance and ages, ranging from Roman and Greek to Magna Graecia colonies and local Italic people (Brettii), were identified. Also Roman soils are in places affected by



Fig. 2. Fluvio-lacustrine terraces of Cecita Lake at Piano di Cecita-Cuponello (a), with one archaeological excavation of late Neolithic to early Eneolithic age (b). Bowtie-shaped lithic artefact representing a weight for fishing net (Piano di Cecita-Cuponello) (c) and early Eneolithic pottery vases at Campo S. Lorenzo site (d). Roman stone wall of Republican age overlying a buried late Neolithic to early Eneolithic soil (e) and kiln for pitch production (f) at Forge di Cecita site (Superintendence of Archaeological Heritage of Calabria – Soprintendenza per i Beni Archeologici della Calabria, Ufficio Territoriale della Sila, Crotone, Italy).

various historical to modern ploughing traces, which often make quite difficult both an archaeostratigraphic and a pedostratigraphic distinction between Republican and Imperial facies, frequently mixed by long-term erosive/depositional and pedogenetic processes. Further details on archaeological site description, findings and chronology are available in Marino and Taliano Grasso (2008, 2010).

4.2. Field features

The three soil profiles studied in this work are located in the two archaeological excavations of the Neolithic/early Eneolithic (soil profile PC) and of the Roman epoch (profiles Arch 1 and Arch 2) on Piano di Cecita-Cuponello and Forge di Cecita terraces, respectively (Figs. 1b and 3). All soils in the archaeological sites display one or more brown (10 YR 4/3–5/3) to dark brown (10 YR 2/2) (when moist) A horizons with typical andic-like field features, such as silt to sandy loam texture, high porosity, high water holding capacity near saturation and good drainage conditions, friable and fluffy consistence, high smeariness, low bulk density, and weak to moderate thixotropy (cf. Cinque et al., 2000; Terribile et al., 2007; Scarciglia et al., 2008). In places, they show repeated traces of ancient to modern ploughing, affecting topsoils (Ap) or sealed in subsurface A horizons. In particular, the late prehistoric soil profile is shallow and sandy loam-textured. It consists of a well-structured (small to coarse angular blocky with prismatic trend), brown A horizon, overlying a dark yellowish brown Bw horizon (Fig. 3a), developed on alluvial sands with occasional skeletal fraction (subrounded fine gravel) of granitic to metamorphic origin. Scarce clay coatings occur in the A horizon, whereas occasional sub-vertical, elongated infillings of humus-rich, brown soil material characterize the underlying pedogenetic horizon. The Roman soil profiles are poorly to moderately deep, with a surface Ap horizon (extremely thin in Arch 1, where a tabular structure can be locally observed in addition to subangular blocky aggregates) and a sub-surface A horizon (Fig. 2b, c). The latter exhibits scarce clay coatings in pores and rare to occasional redox pedofeatures (reddish yellow and black Fe–Mn mottles), probably due to a transient oscillating, perched water table. These horizons are sandy loam in texture, and include subrounded, granitoid fine gravel. At the bottom of soil

appear to form sheet-like units represented by massive conglomerates, suggesting high energy, stream driven depositional events. An additional soil profile in the Roman excavation of Forge di Cecita displays a brown humic horizon (Ab) referred to the late Neolithic/early Eneolithic and developed on coarse fluvial gravel. It is buried by a Roman stone wall of Republican epoch (Fig. 2e), which in turn underlies a brown surface A horizon of Roman age. The main morphological features of these soil horizons are quite similar to those described in the distinct late Neolithic/early Eneolithic and Roman soil profiles, respectively. None of above soil horizons reacted after HCl (10% solution) test on soil matrix. Millimetric to centimetric black charcoal fragments often occur within the soil matrix of the humic horizons. No evidence of volcanic parent material was found in these soils at field scale.

4.3. Chemical and physical analyses

Table 1 reports results of physical and chemical analyses of the studied soils. Particle size analysis shows that all soil horizons from the archaeological sites are dominated by coarse fractions (mainly sand and subordinate silt) with very low clay content ($\leq 8.4\%$ in the Roman soils but never exceeding 18% as in the Neolithic/Eneolithic soil profile). Organic matter is generally high, with values always between 4.9% and 6.5% except in the Bw horizon of profile PC, where it reaches 3.4%. Soil reaction is generally moderately to slightly acid in all soil horizons, reaching a minimum pH(H₂O) value of 5.63 in sample Ap from profile Arch 2. In all soil samples pH(NaF) is always higher than 10. Electrical conductivity is on the whole low, ranging from 11.5 to 26.0 $\mu\text{S}/\text{cm}$ in Roman soils and slightly increasing in Neolithic/Eneolithic horizons, with values between 31.8 and 47.7 $\mu\text{S}/\text{cm}^{-1}$. Total CaCO₃ in the fine earth fraction is always null, except in the A horizon of the Roman profile Arch 1, where it reaches 2%. CEC is moderate to low in the Neolithic/Eneolithic soil horizons (13.1–19.3 $\text{cmol}(+)/\text{kg}^{-1}$), whereas its values are high in Roman soils (between 30.2 and 31.3 $\text{cmol}(+)/\text{kg}^{-1}$). Exchangeable bases are low in all samples and the exchangeable complex is always undersaturated. Higher amounts (and higher exchangeable Ca, in particular) occur in Roman soils than in the Neolithic/Eneolithic one.

Table 1

Physical and chemical features of the archaeological soil profiles. E.C., electric conductivity; O.M., organic matter; C.E.C., cation exchange capacity; Ca, Mg, K, Na, exchangeable bases.

Archaeological ages	Soil profile	Soil horizon	Particle size distribution			pH (H ₂ O)	pH (NaF)	E.C. $\mu\text{S}/\text{cm}$	CaCO ₃ %	O.M.%	C.E.C. $\text{cmol}(+)/\text{kg}$	Ca $\text{cmol}(+)/\text{kg}$	Mg $\text{cmol}(+)/\text{kg}$	K $\text{cmol}(+)/\text{kg}$	Na $\text{cmol}(+)/\text{kg}$
			Sand %	Silt %	Clay %										
Roman Age	Arch 1	A	66.1	27.9	6.0	5.99	10.65	11.5	2	6.1	31.3	4.7	1.2	3.4	2.6
	Arch 2	Ap	64.5	27.5	8.0	5.63	10.17	26.0	–	6.4	30.2	4.6	1.4	3.5	3.3
	Arch 2	A	64.1	27.5	8.4	6.19	10.53	15.1	–	4.9	30.7	4.8	1.3	3.6	2.3
Neolithic	PC	A	56.9	27.1	16.0	6.21	11.00	31.8	–	6.5	19.3	2.9	0.1	0.1	0.2
	PC	Bw	69.6	12.4	18.0	6.52	10.85	47.7	–	3.4	13.1	0.9	0.0	0.1	0.1

profile Arch 1, a >20-cm thick gravel layer (R/C) occurs beneath an abrupt lower boundary of proper soil horizons. It consists of pebble- to cobble-size clasts of granitic and metamorphic rocks, subrounded. They are moderately to poorly sorted and display a clast-supported texture. Matrix content is generally less than 25% and consists of a (yellowish) brown sandy material. Conglomerate fabric is disorganized, although a preferred clast orientation is observed in places. The longest a-axes of some elongate clasts are parallel to paleoflow (eastward on average) directions. Grading is absent but crude inverse grading locally occurs. Conglomerates

4.4. Clay mineralogy

XRD analysis permitted to identify the main clay mineral assemblage in each soil horizon. These results are strongly consistent with the clay mineralogy of non-archaeological soil profiles in the surrounding area, also belonging to the above Cecita Lake geosol (Scarciglia et al., 2008). All samples include halloysite/kaolinite and illite, with vermiculite and/or chlorite, often in traces (Fig. 4). The 1:1 phyllosilicate phases were identified on the basis of the basal reflections at 0.71–0.72 nm, coupled with a weak

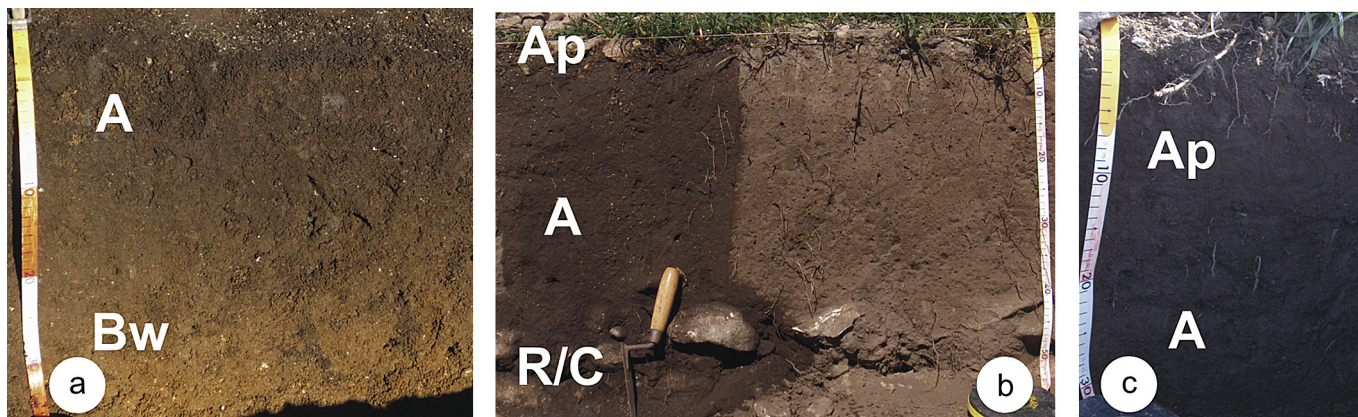


Fig. 3. Soil profiles in the archaeological excavations: late Neolithic/early Eneolithic soil profile (PC) at Piano di Cecita-Cuponello site (a); Roman soil profiles Arch 1 (b) and Arch 2 (c) at Forge di Cecita site.

0.358 nm peak, that completely collapsed (or strongly decreased, see below) after thermal treatment at 550 °C. Asymmetric and sometimes broad 0.7 nm peaks (broader in horizons A and Bw of soil profile PC) support a major presence of dehydrated 0.7 nm-halloysite (over kaolinite) or disordered kaolinite. The hydrated 1 nm-halloysite form ($d = 1.00\text{--}1.03$ nm) was identified thanks to the typical 0.34 nm peak and a partial decrease in intensity of the 1 nm peak (also diagnostic of illite, see below) with consequent reinforcement of the 0.7 d-spacing after heating at 105 °C. Illite was recognized by the reflections at 1.00–1.03 nm and 0.34–0.35 nm (the 0.49–0.51 nm peaks often being poorly recognizable within the background). These peaks persisted after any treatment up to the 550 °C heating, thus supporting the coexistence of illite with hydrated halloysite (see above). Basal reflections at 1.43–1.45 nm, identified on Mg-saturated specimens, indicate the presence of both vermiculite (when they contracted to and reinforced the intensity of the 1.0 nm peak after heating at 335 °C, and disappeared at 550 °C) and/or chlorite (when they were maintained after all treatments). The persistence of the 7.2 nm reflection, though affected by a significant decrease in intensity after heating at 550 °C (indicating above halloysite or kaolinite collapse), coupled with the occurrence of the 0.47 nm and 0.354 peaks, point to the occurrence of some chlorite. No expansion affected the 1.4 nm-peaks after ethylene-glycol solvation, which excludes the presence of smectite components.

Some of these phyllosilicate minerals were also detected in infrared spectra (Fig. 5). Typical diagnostic peaks of halloysite and/or kaolinite were identified at 3696 and 3622 cm^{-1} (O–H stretching vibrations) and sometimes at 3650 or 3656 cm^{-1} (cf. van der Marel and Krohmer, 1969), coupled with the 910–912 cm^{-1} band, the doublet at 796 and 742 cm^{-1} (often poorly expressed) and variably defined bands or simple shoulders at 1035 and 1102 cm^{-1} (this double silica peak being typical of halloysite; e.g. Meijer et al., 2007). Such diagnostic absorbance patterns of 1:1 phyllosilicate clays appear on the whole more developed in soil horizons A and especially Bw of the Neolithic/Eneolithic soil profile. The presence of illite with absorbance bands at 3622, 821 and 754 cm^{-1} (more

easily detected in the same Bw horizon) is probably obliterated by the halloysite spectrum. Although difficult to unravel in multi-phased samples, IR spectra permitted identification of low amounts of short-range order components, such as allophane and/or imogolite. Monomeric (in addition to polymerized) silica can be supposed on the basis of broader and asymmetric Si–O vibrations towards wavelengths <1000 cm^{-1} , where shoulders around 965 and/or 946 cm^{-1} are observed in all A horizons of both Roman soils and at a minor extent of the Neolithic/Eneolithic one. These results suggest the occurrence of some imogolite and/or proto-imogolite (cf. Dahlgren et al., 1993; Meijer et al., 2007). In addition, other small absorbance bands of short-range order aluminosilicates occur at 690, 592, 570 and/or 560 cm^{-1} (Basile-Doelsch et al., 2005; Meijer et al., 2007). In all samples a broad band of absorbance in the range of 3700–3000 cm^{-1} , composed of stretching vibrations of hydration and adsorbed water, is on the whole poorly expressed, typical of both SROM and phyllosilicates.

4.5. Selective extractions

Results from selective extractions, together with some geochemical indices and the allophane and ferrihydrite contents calculated on their basis, are reported in Table 2. The ammonium oxalate extractable forms of aluminium, silica and iron (related to amorphous components or short-range order minerals) are on the whole low in all samples for each element, all of them being always <1 , with extremely low amounts of Si_0 . They are very to moderately homogenous among soil samples for Si_0 and for Al_0 and Fe_0 , respectively. The Na-pyrophosphate extracted aluminium (Al_p), estimating the amounts of active Al related to organic components, displays a little more variable values among different soil horizons, that are always lower than Al_0 . The ICOMAND index $\text{Al}_0\% + 0.5 \text{Fe}_0\%$ is rather low, as a whole, and ranges from 0.80 to 1.19%. The ratio Al_p/Al_0 is always ≤ 0.7 , with the lowest value (0.3) in the Bw horizon of soil profile PC, whereas the index $(\text{Al}_0 - \text{Al}_p)/\text{Si}_0$ is on average 3.3 with slight variations among different soil horizons.

Table 2
Data from selective extractions, related geochemical indices and SROM content in the archaeological soil profiles. Fe_0 , Al_0 , Si_0 , ammonium oxalate-extracted iron, aluminium, silica; Al_p , sodium pyrophosphate-extracted aluminium ($\text{Al}_0 - \text{Al}_p$)/ Si_0 index is given as a molar ratio.

Archaeological ages	Soil profile	Soil horizon	Fe_0 %	Al_0 %	Si_0 %	Al_p %	$\text{Al}_0 + 0.5 \text{Fe}_0$ %	$(\text{Al}_0 - \text{Al}_p)/\text{Si}_0$	Al_p/Al_0	Allophane %	Ferrihydrite %
Roman Age	Arch 1	A	0.50	0.92	0.10	0.61	1.17	2.96	0.7	1.2	0.8
	Arch 2	Ap	0.66	0.86	0.12	0.44	1.19	3.59	0.5	2.3	1.1
	Arch 2	A	0.35	0.63	0.08	0.34	0.80	3.36	0.5	1.3	0.6
Neolithic	PC	A	0.58	0.84	0.12	0.45	1.13	3.25	0.5	1.8	1.0
	PC	Bw	0.35	0.64	0.13	0.21	0.82	3.34	0.3	2.0	0.6

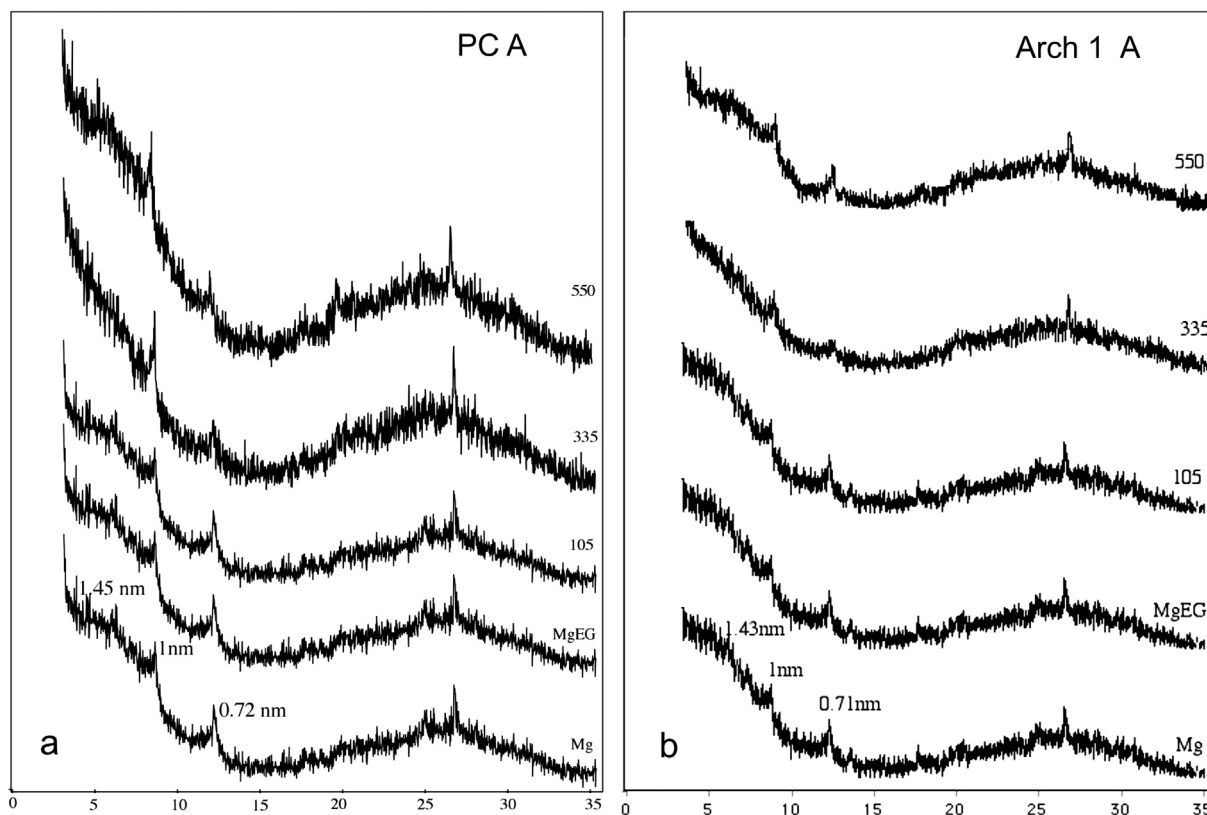


Fig. 4. XRD patterns of clays from A horizons of soil profile PC (a) and soil profile Arch 1 (b).

The allophane content of both late Neolithic/early Eneolithic and Roman soil horizons is relatively low, ranging from 1.25% to 2.01% and from 1.35% to 2.29%, respectively. Therefore very comparable values in the older and younger soils occur. Similarly, the amount of ferrihydrite is poor and comparable between the pre-historic and Roman profiles, always resulting equal to or lower than 1.1%. The highest contents of both allophane and ferrihydrite were estimated in the Ap horizon of the second Roman soil profile (Arch 2).

4.6. Micromorphological features: optical and scanning electron microscopy

The skeletal fraction identified in thin sections is common to abundant in all soil horizons, with higher amounts in the Bw horizon of the Neolithic/Eneolithic soil. It consists of granite and minor gneiss or phyllite rock fragments, coupled with plenty of single quartz, feldspar and mica grains, as expected from the nature of underlying sediments and dominant bedrock in the surroundings (Scarciglia et al., 2005a, 2005b). Mineral surfaces appear weakly to severely weathered in all soil horizons.

Soil microstructure is often very variable in space and ranges from massive and particularly dense (mainly in the Ap horizon of soil profile Arch 2 and A of profile PC) to highly porous and aerated granular/crumby, up to rare single-grain, or (sub)angular blocky (Fig. 6a). In places, the latter is incomplete, despite well-developed but not intersecting planar pores. Both in Neolithic/Eneolithic and Roman A horizons occasional subrounded to subangular blocky clods were observed (Fig. 6b). They are a few millimetres wide, and consist of denser, less porous and a little darker soil material than surrounding matrix and aggregates. Irregular discrete pores to elongated channels (faunal passages) are frequent in all samples.

All A horizons frequently display unaltered to moderately decomposed vegetal tissues, and rare to occasional (more abundant in Roman soils) black charcoal fragments (200 μm to 2–3 mm in size) (Fig. 6c).

The dark brown matrix always exhibits a dominant optically isotropic and subordinate weakly anisotropic behaviour, with scarce and small anisotropic domains, in crossed polarized light (XPL) (Fig. 6d). Only in the Bw horizon of soil profile PC a moderately anisotropic matrix is observed in places. It locally includes some clusters of subrounded to subangular blocky peds with isotropic behaviour in XPL, characterized by humus-rich, dark brown matrix (Fig. 6e).

Overall rare to occasional microlaminated clay coatings occur, mainly all around skeletal grains (Fig. 6f and g). They are a little more abundant in late Neolithic/early Eneolithic (3–5%, up to 8–10% in the Bw horizon of soil profile PC) than in Roman soil horizons ($\leq 2\%$). Their colour is yellow to brownish-yellow, in places superimposed by red Fe-oxide staining. Typical smooth-banded to slightly grainy or intensely speckled extinction patterns observed in XPL indicate a progressive loss of optical anisotropy related to the original clay particle iso-orientation upon illuviation and therefore represent post-emplacment degeneration features with more random rearrangement of clay particles (FitzPatrick, 1984). An additional thin section obtained from the late Neolithic to early Eneolithic Ab horizon, buried beneath the Roman soil and associated building stones (see section on field soil features), displays very similar micromorphological features to those just described in the representative late Neolithic/early Eneolithic soil profile, degenerated clay coatings included.

Occasional silt or silty-clay coatings with a microlaminated, sorted and graded internal fabric occur in the Neolithic/Eneolithic A horizon (Fig. 6h). They are elongated or curved and locally

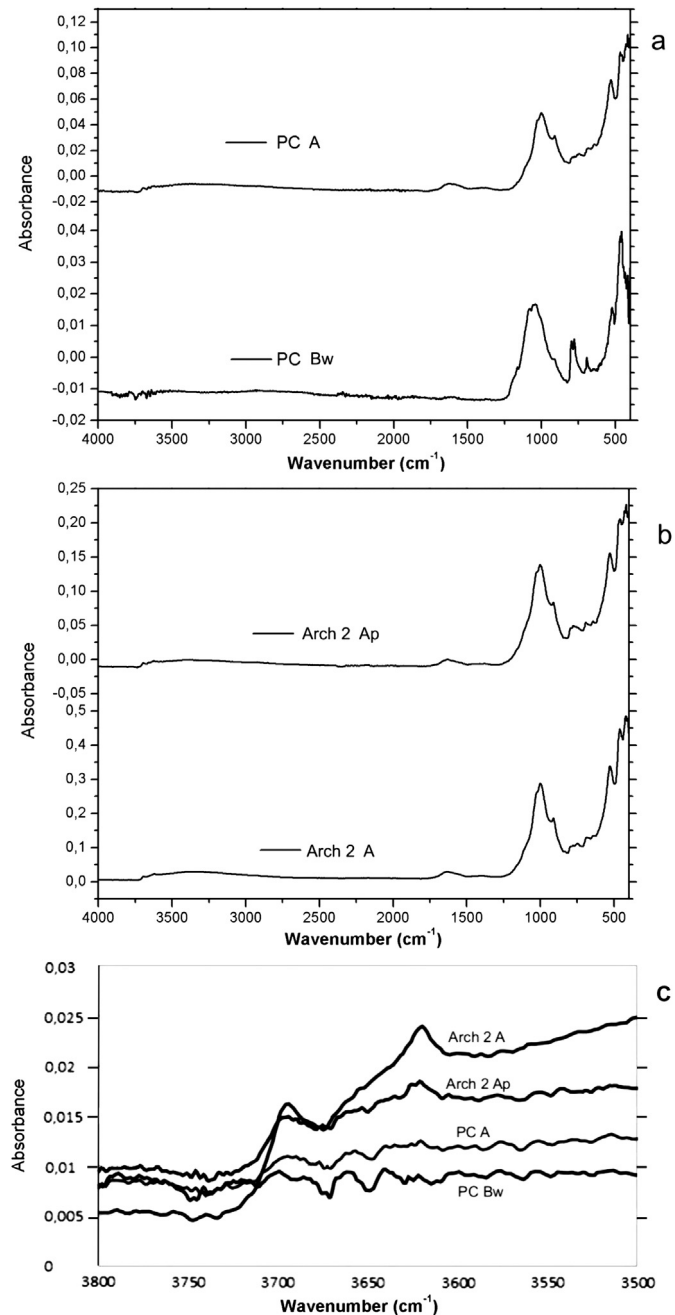


Fig. 5. FT-IR spectra of the clay fraction from soil horizons of profiles PC (a) and Arch 2 (b). A zoom of the higher wavelength range of all spectra (c).

fragmented into two or more segments by sharp fractures. Optically anisotropic, striated clay domains may occur (in XPL), parallel to their outline.

SEM-EDS analysis on the same thin sections permitted identification of scarce and extremely small volcanic micropumices and shards (vesiculated and cuspidate glass fragments, respectively), not detected at field or optical microscopic scales. They range between about 20 and 200 μm in size, are included within the soil matrix of all A horizons from both prehistoric and Roman soils (whereas they lack in the Neolithic/Eneolithic Bw one), and display varying degree of weathering. Based on their rather homogeneous chemical composition (assessed on fresh, unaltered portions of samples and reported in Table 3), rich in silica (72–75%) and with

an alkali content ($\text{Na}_2\text{O} + \text{K}_2\text{O}$) \approx 8–9%, they can be classified as rhyolites.

Table 3

Chemical composition of glass fragments from the studied soil horizons obtained by SEM-EDS analysis.

Sample	SiO ₂ %	TiO ₂ %	Al ₂ O ₃ %	FeO %	MgO %	CaO %	Na ₂ O %	K ₂ O %	Cl ₂ O %
Arch2 Ap	74.0	0.3	13.7	1.8	0.4	0.8	4.0	4.6	0.5
Arch2 Ap_01	72.1	0.2	15.4	2.1	0.6	0.6	4.4	4.4	0.4
Arch2 Ap_02	73.9	0.1	14.1	2.0	0.5	0.6	3.9	4.6	0.3
Arch2 Ap_03	73.5	0.2	14.6	1.7	0.5	0.6	3.7	5.0	0.3
Arch2 Ap_04	73.6	0.2	14.5	1.8	0.4	0.6	4.1	4.4	0.3
Arch2 Ap_05	71.6	0.2	16.7	2.1	0.7	0.6	3.9	3.9	0.3
Arch2 Ap_06	73.8	0.1	14.9	1.9	0.6	0.6	3.4	4.4	0.3
Arch2 Ap_07	74.2	0.2	13.7	2.1	0.4	0.7	3.5	5.0	0.3
Arch2 Ap_08	74.1	0.2	13.7	2.0	0.3	0.8	4.2	4.4	0.3
Arch2 Ap_09	74.3	0.0	13.9	1.4	0.3	0.7	4.1	4.9	0.4
Arch2 A_001	74.7	0.1	13.6	1.8	0.2	0.7	3.7	4.8	0.4
Arch2 A_0010	74.6	0.1	14.5	1.7	0.5	0.7	3.4	4.3	0.3
Arch2 A_0011	74.8	0.1	13.9	1.7	0.3	0.7	3.7	4.6	0.4
Arch2 A_002	74.3	0.2	14.0	1.7	0.3	0.6	4.1	4.5	0.4
Arch2 A_003	74.9	0.1	13.9	1.5	0.3	0.5	4.1	4.5	0.3
Arch2 A_004	74.4	0.1	14.0	2.1	0.3	0.6	3.7	4.5	0.3
Arch2 A_005	74.6	0.1	13.8	1.7	0.3	0.6	4.2	4.4	0.2
Arch2 A_006	74.4	0.2	13.9	1.6	0.4	0.7	4.0	4.5	0.4
Arch2 A_007	74.9	0.1	13.7	1.7	0.3	0.7	3.9	4.5	0.3
Arch2 A_008	74.9	0.2	13.8	1.7	0.3	0.6	3.7	4.5	0.4
Arch2 A_009	74.1	0.1	14.2	2.1	0.3	0.6	3.6	4.6	0.3
PC A_0011	73.4	0.3	14.3	2.7	0.5	0.8	2.4	5.3	0.4
PC A_0012	72.7	0.2	14.3	2.3	1.0	0.6	3.9	4.6	0.4
PC A_0013	73.2	0.1	14.6	2.4	1.1	0.6	3.9	3.9	0.2
PC A_0014	73.3	0.2	14.0	1.8	1.1	0.7	4.1	4.6	0.3
PC A_001	74.2	0.2	14.2	1.7	0.4	0.7	4.5	3.9	0.3
PC A_0010	73.9	0.3	14.1	1.8	0.5	0.7	3.9	4.5	0.3
PC A_002	74.9	1.0	13.5	1.7	0.3	0.7	3.9	4.5	0.4
PC A_003	73.4	0.3	13.9	2.0	0.9	0.8	3.8	4.6	0.4
PC A_004	71.8	0.6	13.3	3.9	0.2	1.3	1.6	6.8	0.5
PC A_005	74.7	0.2	13.5	2.0	0.3	0.9	3.7	4.4	0.4
PC A_006	74.8	0.2	13.6	1.5	0.4	0.7	4.2	4.4	0.4
PC A_007	74.3	0.2	13.8	1.8	0.4	0.9	3.4	4.8	0.4
PC A_008	74.6	0.1	13.9	1.9	0.4	0.8	3.5	4.4	0.4
PC A_009	74.0	0.2	14.2	1.7	0.4	0.7	4.0	4.5	0.4

4.7. Soil charcoal analysis

Results of the charcoal analysis are summarized in Fig. 7. Soil charcoals from the late Neolithic/early Eneolithic profile show the dominance of a mixed deciduous forest with *Quercus* deciduous type, *Populus* and *Carpinus*, along with scarce amounts of *Juniperus* and *Pinus sylvestris* group. On the contrary, *P. sylvestris* group prevails among charcoals in the Roman soils. Very few charcoals of deciduous *Quercus* occur only in the A horizon of soil profile Arch 2. In its topsoil horizon Ap, small amounts of *Prunus*, *Rosaceae* and *F. sylvatica* are present together with dominant *P. sylvestris* group, which represents the only *taxon* identified in the A horizon of profile Arch 1.

5. Discussion

Most of above geopedological data show a number of analogous features among the studied soil profiles of different archaeological periods (late Neolithic to early Eneolithic and Roman epoch), but also some peculiar differences. In particular, the main dissimilarities suggest a bipartite pattern through time of the Cecita Lake geosol in the archaeological soils. Both similarities and differences, coupled with corresponding results of soil charcoal analysis, revealed to be useful tools for reconstructing the main soil-forming processes and environments and their changes in response to the

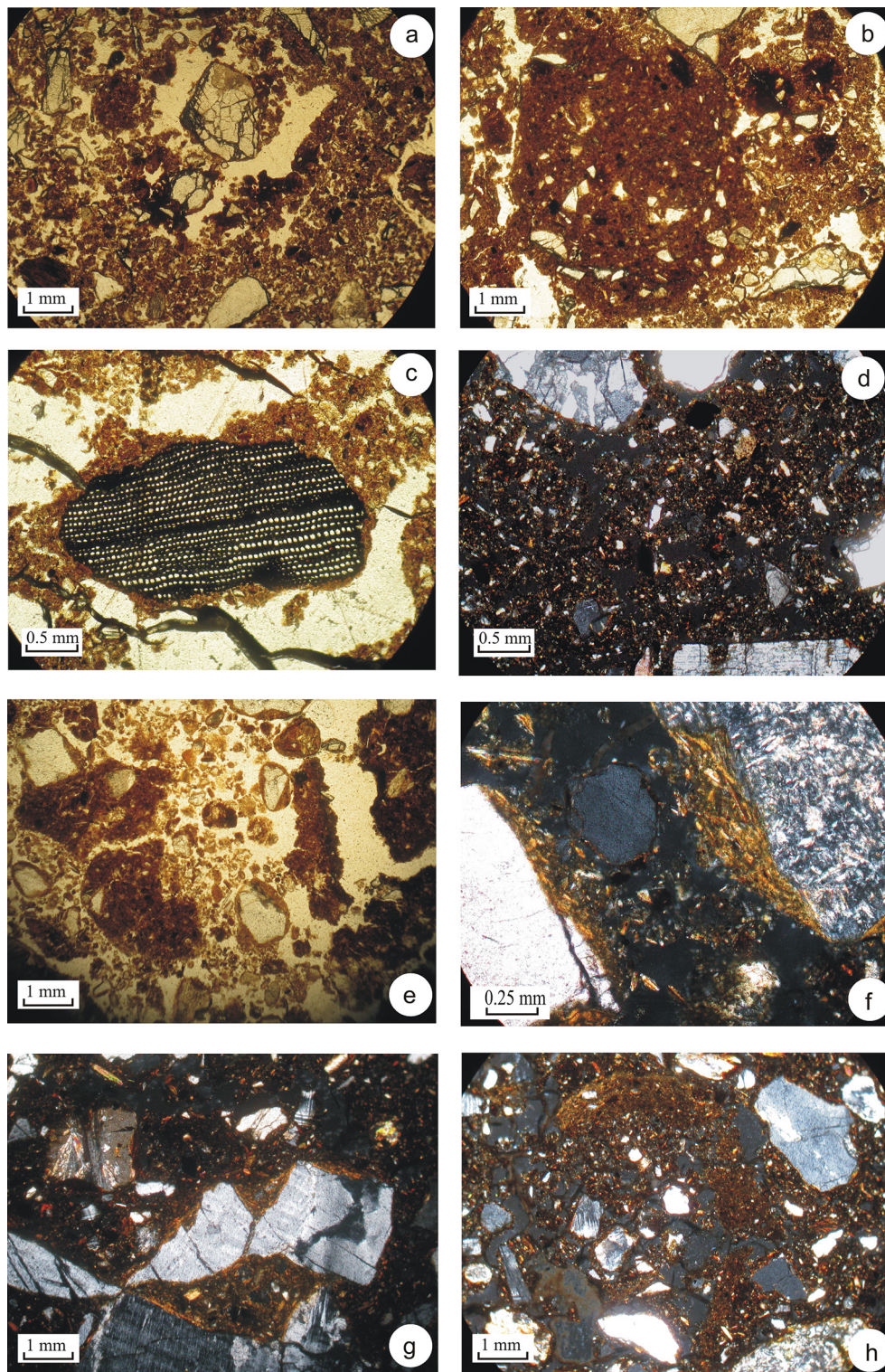


Fig. 6. Microphotographs of: (a) varying soil matrix and microstructure in the A horizon of soil profile Arch 2 (plane polarized light – PPL); (b) subrounded clod with denser and darker soil material than surrounding matrix and peds (A horizon, soil profile Arch 1, PPL); (c) charcoal fragment of coniferous wood (probably *Pinus nigra* subsp. *laricio*) enclosed in the soil matrix of the A horizon of profile Arch 1 (PPL); (d) dominant optically isotropic matrix with scarce and small anisotropic domains (A horizon, soil profile Arch 2, XPL); (e) dark brown, humus-rich subangular blocky peds within a lighter-coloured crumbly to single-grained microstructure in the Bw horizon of soil profile PC (PPL); (f) degenerated clay coatings with dominant grainy to smooth-banded extinction patterns (XPL) in the Bw horizon of soil profile PC (f) and the A horizon of profile Arch 2 (g); (h) curved, elongated and broken silty-clay coatings showing a microlaminated, sorted and graded internal fabric with optically anisotropic, striated clay domains (A horizon, soil profile PC, XPL). (For interpretation of the references to colour in this figure legend, the reader is referred to the web version of this article.)

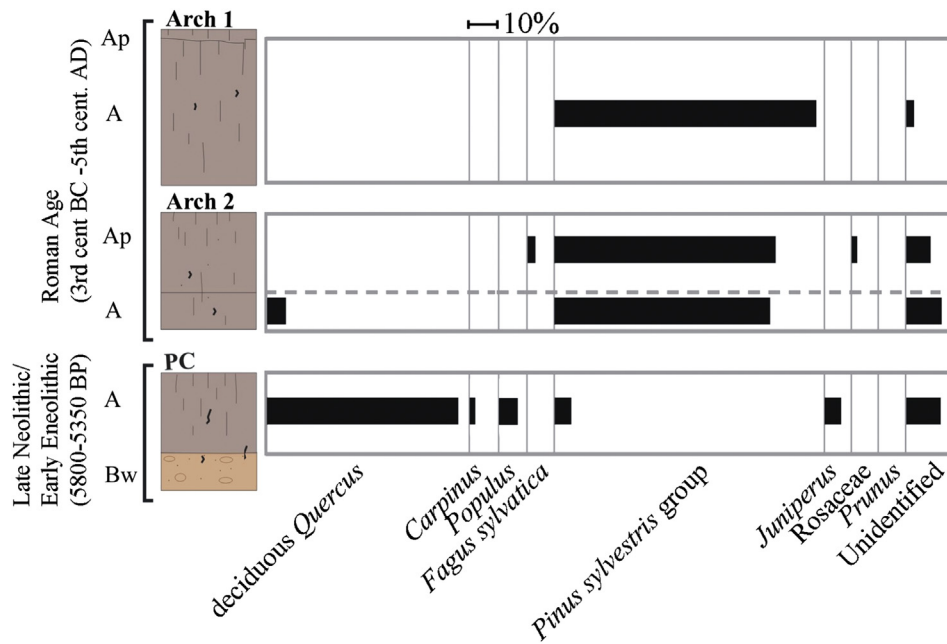


Fig. 7. Results of charcoal analysis in the archaeological soils of Cecita Lake.

major climatic and ecosystem changes occurred during the Holocene on the Sila plateau, including the effects of human pressure (Fig. 8).

The fact that the studied soil profiles represent mainly surface soils implies that some imprint of recent pedogenesis and some post-pedogenic disturbance by anthropogenic activities are probably recorded. However, their bipartite behaviour is still evident, though the timing of some post-prehistoric pedogenetic processes is difficult to unravel. In this respect, the reliability of the main pedological features and laboratory data is strongly supported by:

- (i) the distinct archaeological content and the lateral spatial continuity of the archaeological layers in the excavations where the soil profiles were dug, which include preserved in situ remains of different epochs and permit a clear separation of the late Neolithic/early Eneolithic from the Roman soil horizons (at one site the late prehistoric soil is also buried by the Roman one);
- (ii) the preservation of the main diagnostic pedofeatures (e.g. clay coatings) in the different horizons and the lack of papules or pedorelicts;
- (iii) the recurrence of a similar bipartite pattern between early-mid and late Holocene soils in another archaeological site of southwestern

Soil profiles	Archaeological period / Age	Geomorphological and pedological evidence	Paleoclimatic/ environmental changes	Vegetation dynamics	Paleoclimatic/ environmental changes
Arch 1	Republican to late Empire Roman Age (3rd cent. BC - 5th cent. AD)	Dominant SROM	Poorly contrasted humid climate	Dominant pine forest	Drought phase(s) and/or human impact (agriculture, deforestation)
Arch 2		Decrease of clay illuviation	Temperature decrease under humid conditions or drought phase(s)		
PC	ca. 3000 a BP	Soil erosion, sedimentary aggradation, soil burial	Drought phase(s) and/or human impact (agriculture, deforestation)	Substitution of oak forest with pine forest	Warm and humid climate with some seasonal contrast (climatic optimum)
	Late Neolithic/ early Eneolithic (5800-5350 a BP)	Dominant phyllosilicates Degenerated clay coatings (relict clay illuviation)	Warm and humid climate with some seasonal contrast (climatic optimum)	Dominant oak forest	

Fig. 8. Synthetic scheme of Holocene paleoenvironmental/climatic changes reconstructed in archaeological soils at Cecita Lake (see text for details).

Calabria about 130 km far from Cecita Lake (Bernasconi et al., 2010; Pelle et al., 2013), pointing to a wider, possibly regional, significance of this change; (iv) the presence of similar pedofeatures in the Neolithic soil of another site in northwestern Calabria, overlain by different ones that testify for changing pedoenvironments (Scarciglia et al., 2009); (v) the concurrent changes of soil features and charcoal content between Neolithic/Eneolithic and Roman times; (vi) the additional evidence of a drastic shift in the landscape response to this transition clearly highlighted by sedimentary aggradation. More detailed considerations on some of these major items are discussed in the following subsections.

5.1. Evaluation of andic properties and volcanic input

Geochemical results from selective extractions permitted an evaluation of andic properties in the studied soil profiles. High pH(NaF) values (always ≥ 10.2) indicate the presence of free Al incorporated into short-range order minerals and/or humus–aluminum complexes (Fieldes and Perrott, 1966; IUSS Working Group WRB, 2007; Soil Survey Staff, 2010). The occurrence of some amounts of these components is also supported by the ICO-MAND index, which is lower than 2% in all samples ($Al_o\% + 0.5 Fe_o\% \leq 1.19\%$), but always exceeds the minimum requirement (0.4%) for andic properties (cf. IUSS Working Group WRB, 2007; Soil Survey Staff, 2010). The moderate amount of oxalate extractable Al and Fe shown by the index values (in turn indicating vitric properties, sensu IUSS Working Group WRB, 2007) can be considered a proxy for lower amounts of poorly-crystalline pedogenetic minerals. They are comparable to values measured in the widespread geosol of Cecita Lake (Scarciglia et al., 2008). Coherently, values of Si_o always $< 0.6\%$, coupled with Al_p/Al_o ratios $\geq 0.5\%$ (except in the Bw horizon of soil profile PC), indicate that most samples display alu-andic properties (sensu IUSS Working Group WRB, 2007). This means that Al pool complexed by organic substances prevails over Al entering the crystal lattice of SROM (García-Rodeja et al., 2007), as in non-allophanic Andisols (Nanzyo et al., 1993). The molar ratio of Al:Si in short-range order aluminosilicates was estimated using the index $(Al_o - Al_p)/Si_o$, which corrects for organically bound aluminium (Parfitt and Wilson, 1985). It shows values on average around 3.3 (usually being in the range between 1 and 2 in allophane and imogolite; Parfitt and Henmi, 1982; Dahlgren et al., 1993), thus supporting the dominance of Al-rich (versus Si-rich) poorly-crystalline components. Al:Si ratios > 2 may account for an excess of other Al-phases than mere SROM components extracted by acid oxalate: above humus–aluminum complexes, some gibbsite or hydroxy-Al-interlayered clay minerals, opaline silica (Dahlgren et al., 1993; García-Rodeja et al., 2007; Meijer et al., 2007). The allophane content calculated on the basis of the $(Al_o - Al_p)/Si_o$ ratio, is on the whole low and ranges between 1.2 and 2.3%, which is in the range of other European soils (García-Rodeja et al., 2007). These results, along with the contemporary lower amount of ferrihydrite (always $\leq 1.1\%$), are consistent with above considerations and confirm an overall low quantity of short-range order minerals in the investigated soils. Such evidence is likewise corroborated by mineralogical data. In fact, the presence of some SROM is shown by FT-IR spectroscopy. These poorly-crystalline phases occur in all soil horizons together with phyllosilicate clays, which are conversely higher especially in the lower horizon of the late Neolithic to early Eneolithic soil profile PC. Phyllosilicates are in turn clearly identified by X-ray diffraction analysis. In particular, halloysite (possibly often coupled with kaolinite) is ubiquitous in all soil profiles, as indicated by XRD patterns and infrared spectra, with fairly distinguished diagnostic IR peaks in sample Bw of profile PC. Both allophanic components and halloysite represent typical weathering products of volcanic

parent materials (e.g. Dahlgren et al., 1993; Vacca et al., 2003; Colombo et al., 2007; Gérard et al., 2007) including glass, clearly identified using electron microscopy. On one hand, more abundant phyllosilicates than SROM in the Neolithic/Eneolithic Bw horizon very likely indicate a stronger contribution of neoformed clay minerals from underlying granite parent rocks than from wind-blown volcanic glass. In particular, it is well-known that kaolinite and vermiculite are common weathering products of feldspars and micas (e.g. Barnhisel and Bertsch, 1989; Kretzschmar et al., 1997; Taboada and García, 1999; Sequeira Braga et al., 2002), whereas chlorite represents a typical accessory primary mineral of granitoids. A mixed nature of parent materials as sources of different types of neogenic mineral phases in the soils of the Sila uplands was already highlighted by Scarciglia et al. (2008). Such results are consistent with the lack of micropumices shown by SEM observations in the Bw horizon (late Neolithic/early Eneolithic soil profile), whereas they were found in all the other more recent and/or upper soil horizons, where IR peaks of phyllosilicate clays are less expressed. Possible shifts in (pedo)climatic conditions could have promoted such mineralogical differences (see next subsection). Finally, the dominance of poorly-crystalline components especially in all A horizons is supported by micromorphological analyses. The prevailing isotropic optical behaviour of the soil matrix under crossed polarized light testifies for dominance of short-range order minerals and/or amorphous humic substances. In contrast, the small and generally scarce, anisotropic domains (a little more common in the Bw horizon of soil profile PC) highlight a simultaneous presence of some crystalline clays (relatively more abundant in the same soil profile).

As expected, the rhyolitic chemical composition of the volcanic pumices is similar to that assessed in the Cecita Lake geosol, which indicates a provenance from possibly different late Pleistocene to Holocene eruptions from the Aeolian Islands (Scarciglia et al., 2008). Very likely they represent the equivalent distal, wind-blown products of more proximal fine ashes with rhyolitic composition identified in other Holocene soils along the southern Tyrrhenian coast of Calabria (Bernasconi et al., 2010; Pelle et al., 2013). The most likely volcanic events predating late Neolithic/early Eneolithic and Roman soil formation are the Pollara eruptions (24–13 ka) from Salina (Keller, 1980; Calanchi et al., 1993), those forming the Valle Muria synthem (42–22 ka) and the earliest products (< 11 ka) of the Vallone Fiume Bianco synthem from Lipari (Crisci et al., 1991; Tranne et al., 2002; De Rosa et al., 2003), among which the Gabellotto-Fiumebianco eruption (~ 8.5 ka BP; Zanchetta et al., 2011). As the archaeological soil profiles studied are exposed at topographic surface, the volcanic ash therein included could have been also emplaced by more recent rhyolitic eruptions than corresponding archaeological ages, up to the historical events of Mt. Pilato (AD 800) and Rocche Rosse (AD 1230) from Lipari (Tanguy et al., 2003; Arrighi et al., 2006). Progressive assimilation of micropumices into the soil profiles (possibly encouraged by biological and agricultural activities; see below) and their easy weathering led to a relatively rapid soil buildup. Rates of soil formation were higher than those of simultaneous (though certainly pulsing) volcano-sedimentary input, leading to an almost complete transformation and homogenization of fresh volcanic parent material into the partly formed soil profile, without any clear lithological and pedogenetic discontinuity (cf. accretionary soils, sensu Catt, 1998; Kemp, 1998; and continuous (regular) syn-lithogenic pedogenesis, sensu Tursina, 2009). Surface exposure could have even caused at least partial overprinting of features related to more recent pedogenetic processes (e.g. leaching) over the past ones, and thus possibly obliterated some climatic signals related to the past. This could explain the lack of more marked differences (except some still distinct features already discussed in

this and following subsections) between the soils of the two different epochs.

5.2. Climatic changes

SROM formation is influenced chiefly by macro- and micro-environmental factors (e.g. soil pH, leaching, organic carbon content) together with the mineralogical and physico-chemical composition of parent materials (with consequent different release and availability of Si and Al), in turn controlled by climate, topography, drainage, vegetation, tephra thickness, depth of burial, etc. (cf. Parfitt, 2009). On the whole, their formation is usually promoted by weathering of volcanic ash (glass) under prolonged moisture availability, mainly (but not exclusively) in soils with udic moisture regimes and with good drainage (Duchaufour, 1982; Buol et al., 1989; Parfitt and Kimble, 1989; Shoji et al., 1993). Both short-range order aluminosilicates and halloysite form in Si-rich environments (Parfitt and Wilson, 1985; Dahlgren et al., 1993; Colombo et al., 2007). At the study sites they are strongly enhanced by the weathering of both granite rocks and rhyolitic pumices. Imogolite is more stable than halloysite over a wide range of Si activity, whereas above a certain level of such an activity, halloysite becomes more stable than imogolite (Parfitt, 2009). The above discussed dominance of Al-rich (rather than Si-rich) allophanes, as well as their overall low amount, is consistent with the acidic soil reaction and a relatively low Si content in the soil solution (Parfitt and Kimble, 1989). This could be related to a severe leaching environment (promoted by the high rainfall rates in the study area and the well-drained udic moisture regime of the soils, in turn confirmed by their undersaturated exchangeable complex), that causes Si removal from the soil solution, thus partly inhibiting neogenesis of short-range order aluminosilicates, or a young pedoenvironment (Parfitt and Wilson, 1985; Shoji et al., 1993; Colombo et al., 2007), coherent with the archaeological ages.

As recently reviewed by Parfitt (2009), halloysite can form directly from volcanic glass when Si activity in the soil solution is high, but it is also thought to derive possibly from weathering of allophane in relatively old tephra, under similar silica availability. This transformation is particularly enhanced from Si-rich (rhyolitic) tephric material, as the present case. Proto-imogolite allophane may weather to halloysite following a rearrangement of crystal structures, which only takes place after dissolution and reprecipitation.

The different relative amounts of SROM and phyllosilicates highlighted by geochemical/mineralogical results can be also related to different time spans of soil formation. On the whole higher SROM content in the Roman soils than in the Neolithic/Eneolithic one suggests earlier stages of pedogenic development, as phyllosilicate minerals may also derive from transformation of poorly-crystalline phases. Moreover, SROM vs. phyllosilicates can be also interpreted in terms of climatic and pedoclimatic changes. Actually, allophanic components are favoured by high water availability and free drainage (mainly udic soil moisture regime). In contrast, more seasonally contrasted climatic conditions, such as warm and humid or definitely drier, weakly leached environments (possibly ustic to xeric up to aridic soil moisture regimes), enhance the formation of phyllosilicate clays and specifically halloysite (Parfitt et al., 1984; Dahlgren et al., 1993; Egli et al., 2008). In particular, the presence of dehydrated halloysite together with allophane can be considered as an indicator of climatic changes towards drier environments (Dubroeuq et al., 1998).

The presence of some clay coatings in the Neolithic/Eneolithic soil profile, their ageing and relict (present-day inactive) significance proved by their degeneration features, along with the archaeologically determined soil-age, suggest their formation

during the late early-middle Holocene climatic optimum (cf. Rossignol-Strick, 1999), during which the latest phases of significant clay illuviation are documented across wide mid-latitude European and peri-Mediterranean areas (Catt, 1989; Cremaschi and Trombino, 1998). Emplacement of clay coatings in this period is also recorded in other sites of northern and southern Calabria (Scarciglia et al., 2009; Bernasconi et al., 2010; Pelle et al., 2013), including the nearby non-archaeological, buried pedofacies of the Cecita Lake geosol (Scarciglia et al., 2008). Although clay illuviation may occur under varying climatic conditions with high moisture availability, their higher abundance in the same soil profile PC, where phyllosilicate clay minerals (and specifically halloysite) prevail over SROM components, suggests a warm and humid (pedo) climate characterized by some seasonal contrast. These conditions can enhance clay particle stacking within pores, as a response to capillary water evaporation or evapotranspiration promoted by plant uptake. The presence of *Quercus* deciduous forest strongly supports this interpretation. The decrease of clay coatings in Roman soils was probably a consequence of climate drying, as decreased water availability inhibited clay particle illuviation. Phyllosilicate clays could have at least partly formed after irreversible dehydration of poorly-crystalline aluminosilicates under drier climatic conditions. Various drought phases towards or after the end of the Holocene climatic optimum (about 5.5, 4.2, 3 and 2 ka BP, though with different chronological shifts in their start/end ranges according to peculiar site responses) could have been potentially responsible for such a climate change, as already documented by different proxies, both in Italy and at wider Mediterranean scales (e.g. Frezzotti and Narcisi, 1996; Huntley et al., 1999; Roberts et al., 2001; Sadori and Narcisi, 2001; Allen et al., 2002; Hunt et al., 2004; Bernasconi et al., 2006; Sadori et al., 2008; Costantini et al., 2009; Di Rita and Magri, 2009; Jalut et al., 2009; Peyron et al., 2011; Magny et al., 2012b).

Although probably less straightforward, a different hypothesis could be taken into account to explain the post-Eneolithic decrease of clay coatings recorded in Roman soils, possibly not excluding but coupling above interpretation. At least temporary temperature decrease after the Neolithic age still under humid conditions could have caused a diminished seasonal contrast, that could have been less suited for illuvial clay particle stacking within soil pores, as also observed in a southernmost archaeological site of Calabria (Piani della Corona) located on a coastal terrace close to the town of Palmi (Bernasconi et al., 2010; Pelle et al., 2013). The prevalence of neogenic allophanic products over phyllosilicate clays in the Roman soil horizons with respect to the Neolithic/Eneolithic ones is in agreement with a pedoenvironment characterized by overall prolonged moisture availability. The relevance at a wider spatial scale of this feature is supported by mineralogical/micromorphological data obtained at the Palmi site, where a more pronounced increase of SROM vs. phyllosilicates is recorded at the transition from the late Neolithic to the post-late early Bronze age (Bernasconi et al., 2010; Pelle et al., 2013). This behaviour, which is apparently in contrast with a general drying trend of the late Holocene with respect to its mid part, generally accepted to have been moister (e.g. Jalut et al., 2009; Peyron et al., 2011; Magny et al., 2012b), could be explained by the mountainous environment of the study area (also at present very cool and rainy) and by the orographic barrier effect of the coastal cliff (facing the Tyrrhenian Sea) on rainfall at the Palmi site, respectively, which could have attenuated the efficacy of some drought events recorded in other Mediterranean sites. These results are coherent with repeated phases of higher lake levels recorded during the late Holocene (Dramis et al., 2003; Giraudi, 2007; Giraudi et al., 2011; Magny et al., 2012a), although their timing cannot be resolved in our

soils. Various climatic indicators also highlight the occurrence of late Holocene cool climatic conditions (Sauro et al., 2003; Di Donato et al., 2008). In particular, a persistence of moist conditions throughout the Holocene without any pronounced mid- or late-Holocene aridification trend is documented by vegetation dynamics reconstructed in two lakes from the SE coast and the NE mountain belt of Sicily, southern Italy (Tinner et al., 2009; Bisculm et al., 2012).

5.3. Environmental changes and human impact

Soil charcoal data are generally considered to provide accurate local information on vegetation cover, since charcoal fragments buried in soils are the result of fires in local woody vegetation (Carcaillet and Thion, 1996). The same local, ecological conditions can be reflected also by dispersed charcoal in archaeological horizons resulting from long-term activities and processes (Figueiral and Mosbrugger, 2000). Charcoal data from the archaeological soil profiles at the study sites provided some important insights into environmental changes and human impact.

A severe change from late prehistoric to Roman soils at Cecita is indicated by corresponding soil charcoal data. The Neolithic/Eneolithic vegetation cover, dominated by a deciduous oak forest, is almost completely substituted in Roman epoch by a mountain pine forest of *P. sylvestris* group, which includes *P. nigra*, *P. sylvestris* and *P. mugo*. Although wood anatomy does not allow to reach species-level identification, *P. sylvestris* and *P. mugo* can be ruled out because they do not grow in this region (Pignatti, 1982). In this case we can ascribe these charcoals to *P. nigra* subsp. *laricio*, because this species is an endemic and very widespread tree in the mountain vegetation of Calabria, between 800 and 1800 m a.s.l. (Pignatti, 1982). Above vegetation change testifies for a prominent deterioration of the environment after the Neolithic. In fact, it is very likely that pine colonization should have followed a strong degradation of previous deciduous forest, because *P. nigra* subsp. *laricio* is a pioneer and heliophilous tree, able to colonize open ground (Pignatti, 1982; Quézel and Médail, 2003).

Despite a chronological gap of about three thousand years between the late Neolithic/early Eneolithic and Roman age soil profiles, an overall landscape stability with important soil formation is recorded at Cecita site until about 3 ka BP, at least. This is clearly testified by the nearby pedologic profile (located on the same fluvio-lacustrine terrace), where the latest phases of soil-formation of the analogous, well-developed late Pleistocene–late Holocene soil buried by slope deposits, were dated to that time by radiocarbon (see above Cecita Lake geosol and Scarciglia et al., 2008). As suggested by the same authors, the overlying, younger detrital deposition (which overlies the geosol in other sites of the Sila uplands than the sole surroundings of Cecita Lake) records a drastic change towards geomorphologic instability and strong land degradation since 3 ka BP onward, presumably caused by increasing human pressure, namely forest clearance.

Clear disturbances in forest ecosystems have been recorded since ca. 4000 a BP at Lago Trifoglietti (about 50 km NW from Cecita), where pollen data record a forest reduction that can be related to the combined effects of the mid to late Holocene climate drying and the increasing impact of growing populations (Joannin et al., 2012). In this record it is also interesting to note the scarcity of *Pinus* pollen, which probably occupied extremely restricted surfaces: in this respect we stress the higher spatial resolution of charcoal data able to detect local populations.

Anthropogenic environmental changes during the same periods are documented also in other papers for the same study area

and its surroundings (Sorrison-Valvo, 1993; Dimase et al., 1996) or for other sites in southern and central Italy (e.g. Allen et al., 2002; Sadori et al., 2004; Piccarreta et al., 2011). During Roman times, intense deforestation was carried out in Sila uplands to exploit wood resources for houses, ships and any other building purposes. Certainly, Neolithic people already initiated deforestation (Sorrison-Valvo, 1993), possibly also using slash-and-burn techniques, to gain space for agricultural crops. This is demonstrated by field evidence of multi-story plough traces in the studied archaeological soils, ranging from late prehistoric to modern times. Moreover, the broken, sorted, striated and laminated silt coatings identified in thin sections in the late Neolithic/early Eneolithic A horizon (despite their not univocal and often disputed origin; e.g. Usai, 2001; Kühn et al., 2010) may represent typical agricultans (sensu Jongerius, 1970) or agro-striated b-fabric (cf. Huisman et al., 2009), related to tillage. Each of the internal microfabrics described in such textural pedofeatures can be related to some of the following processes in connection with agricultural activities: shear forces and particle compaction with development of striated laminae (possibly plough-pans), their following rupture and/or disaggregation, and repeated slaking of coarse and fine material from bare, structurally unstable soil surface, with consequent washing of particles through the soil profile to form graded, laminated silt (and silty-clay) coatings (Wilson et al., 2002; Adderly et al., 2010). The occurrence of subrounded to subangular blocky clods of dense soil material in A horizons suggests some disturbance (Huisman et al., 2009) by at least partly post-pedogenic processes. These may have been possibly caused by biological activity or more likely by reworking phenomena linked to cultivation practices. Similar considerations can explain the high heterogeneity of the microstructure observed in thin sections (Adderly et al., 2010) and the coexistence of primary minerals with differential weathering (Pang et al., 2006). The dark brown humic, optically isotropic, subrounded/subangular peds identified at the microscale in the Bw horizon of soil profile PC suggest some reworking of soil material from the overlying A horizon, partly within subvertical tongues possibly left by decayed roots, as indicated by the macroscale humus-rich infillings. Moreover, remnants of subsoil exposed at the ground surface, as the occurrence of clay coatings in typical topsoil (A) horizons suggests, indicating that they are partly truncated by erosion processes, are often documented in old, intensely eroded, cultivated fields (cf. Montgomery, 2007). Finally, some amount of CaCO₃ found in one of the Roman soil profiles can be explained in the context of carbonate-free parent materials of the Sila uplands by modern soil amendment and fertilization superimposed on the ancient soil features.

On the basis of these results, we think that an anthropogenic degradation of the soil-vegetation cover during the Holocene plays a prominent role in the Cecita area, where a mutual superimposition and reinforcement between the effects of climatic changes and those operated by man's activities probably occurred. However, real effectiveness of above drought phases in such a mountainous environment with present-day high rainfall rates and past water availability recorded in various soil features (see previous subsection) is difficult to estimate. We wonder they were probably not strong enough to allow a so severe response of vegetation from deciduous to pine forest after the Neolithic climatic optimum. However, their cyclical repetition during the late Holocene could suggest a sort of "cumulative" effect on the natural environment through time. Among the major drying episodes, the older ones, at 5–5.5 ka BP (Colombaroli et al., 2007; Marchetto et al., 2008) and at 4–4.2 ka BP (e.g. Drysdale et al., 2006; Zanchetta et al., 2012), could have had a mere "preparatory" role in the vegetation shift, because at about 3 ka BP an overall geomorphic stability is still recorded in

the Cecita area (see above). Therefore, it can be supposed that a significant role in such a vegetation change besides the prominent effects of human activities could have been also promoted by one or both the younger drought episodes, i.e. those around 3000 or 2000 years BP.

In an indirect way, the volcanic input concurring to soil formation could have been relevant for environmental changes in the Cecita area. Nutrient availability in the soil ecosystem favored by rapid weathering of volcanic glass (see first subsection of present discussion), coupled with suited climatic conditions, water availability, vegetation cover and accumulation of soil organic matter, probably promoted high soil fertility since late Neolithic times (and even before). These characteristics very likely influenced the choice of the sites in different prehistoric to historical epochs for various settlements and progressively more extensive exploitation of raw materials and any other natural resource for building and people subsistence (stones, land for crops, water, fish, wood and pitch). Land use modifications caused by forest clearance, slash-and-burn and agricultural practices probably also indirectly affected plant diversity and dynamics through time, because significant vegetation changes certainly affected the main properties of the soil (organic matter content and its preservation, soil productivity and nutrient cycling, aggregate stability, exposure to raindrop impact and surface water runoff, soil thickness, drainage and infiltration, etc.) as plant-sustaining natural ecosystem. In turn this soil response, possibly leading to its impoverishment, overexploitation or loss, could have influenced some natural vegetation changes, in a strict mutual feedback mechanism.

6. Conclusions

The multidisciplinary study of Holocene archaeological soils in the upland Mediterranean site of Cecita Lake (Sila massif, Calabria, southern Italy) was revealed to be very powerful for reconstructing mid to late Holocene paleoenvironmental changes in response to climate and human impact. Based on their main features and laboratory results, two distinct environments can be delineated for these epochs. Warm climatic conditions with high water availability and some seasonal contrast characterized the late prehistoric period (during the Holocene climatic optimum), under an oak-dominated (deciduous *Quercus*) forest. These conditions promoted humus accumulation, clay illuviation and phyllosilicate neogenesis (prevailing over short-range order components) in soils, partially developed on very fine, distal volcanic ashes sourced from late Pleistocene to Holocene eruptions of the Aeolian Islands. This phase of overall geomorphological stability was followed by a severe land instability and degradation, presumably caused by mid-Holocene climate drying (evidenced by clay coating decrease) and strongly reinforced by increasing human pressure since the last 3 ka BP, culminated during Roman times (forest clearance and wood exploitation, pitch extraction, field cropping and tillage). Severe anthropogenic disturbance promoted an almost complete substitution of oaks by a pine forest dominated by *P. nigra* subsp. *laricio*. Ongoing soil charcoal analysis on further selected soil profiles will clarify the timing of these vegetation changes. Finally, late Holocene soils record a restoration of overall humid and possibly cooler climatic conditions, indicated by dominance of short-range order aluminosilicates over phyllosilicate clays as neoformed products. This behaviour can be explained by the specific mountainous, very humid environment of the study area, where the effects of possible arid events recorded elsewhere could have been strongly attenuated. The absence of a clear drying trend from the mid to the late Holocene at this site represents a very relevant result in the long-lasting, controversially debated issue of Holocene climate pattern both in Italy and the Mediterranean area.

Acknowledgments

We are grateful to Paola Donato (University of Calabria) for interesting discussion on volcanic sources and to Giuseppe Vecchio, Pier Giorgio Vasta, Mariano Davoli and Valentino Pingitore for their contribution and help in some pedological laboratory analyses and SEM-EDS. We also thank Giovanni Zanchetta (University of Pisa) and two anonymous reviewers for their helpful comments and suggestions.

References

- Adderly, W.P., Wilson, C.A., Simpson, I.A., Davidson, D.A., 2010. Anthropogenic features. In: Stoops, G., Marcelino, V., Mees, F. (Eds.), *Interpretation of Micromorphological Features of Soils and Regoliths*. Elsevier, Amsterdam, pp. 569–588.
- Allen, J.R.M., Watts, W.A., McGee, E., Huntley, B., 2002. Holocene environmental variability – the record from Lago Grande di Monticchio, Italy. *Quaternary International* 88, 69–80.
- Amodio-Morelli, L., Bonardi, G., Colonna, V., Dietrich, D., Giunta, G., Ippolito, F., Liguori, V., Lorenzoni, S., Paglionico, A., Perrone, V., Piccarreta, G., Russo, M., Scandone, P., Zanettin Lorenzoni, E., Zuppeta, A., 1976. L'Arco Calabro Peloritano nell'orogene appenninico-maghebide. *Memorie della Società Geologica Italiana* 17, 1–60.
- Anderson, D.G., Maasch, K.A., Sadweiss, D.H. (Eds.), 2007. *Climatic Change and Cultural Dynamics. A Global Perspective on Mid-Holocene Transitions*. Academic Press, San Diego, p. 575.
- Arrighi, S., Tanguy, J.-C., Rosi, M., 2006. Eruptions of the last 2200 years at Vulcano and Vulcanello (Aeolian Islands, Italy) dated by high-accuracy archeomagnetism. *Physics of the Earth and Planetary Interiors* 159, 225–233.
- ARSSA (Agenzia Regionale per lo Sviluppo e per i Servizi in Agricoltura), 2003. I suoli della Calabria. Carta dei suoli in scala 1:250000 della Regione Calabria. In: *Monografia divulgativa. Programma Interregionale Agricoltura-Qualità – Misura 5*, ARSSA, Servizio Agropedologia, Rubbettino Ed., Soveria Mannelli, Catanzaro, Italy, p. 387.
- Barnhisel, R.L., Bertsch, P.M., 1989. Chlorite and hydroxy-interlayered vermiculite and smectite. In: Dixon, G.B., Weed, S.B. (Eds.), *Minerals in Soil Environments*, second ed. Book Series 1 Soil Science Society of America, Madison, Wisconsin, pp. 729–788.
- Bascomb, C.L., 1968. Distribution of pyrophosphate-extractable iron and organic carbon in soils of various groups. *Journal of Soil Science* 19, 251–268.
- Basile-Doelsch, I., Amundson, R., Stone, W.E.E., Masiello, C.A., Bottero, J.Y., Colin, F., Masin, F., Borschneck, D., Meunier, J.D., 2005. Mineralogical control of organic carbon dynamics in a volcanic ash soil on La Réunion. *European Journal of Soil Science* 56 (6), 689–703.
- Bernasconi, M.P., Chiocci, F.L., Critelli, S., La Russa, M.F., Marozzo, S., Martorelli, E., Natali, E., Pelle, T., Robustelli, G., Russo Ermolli, E., Scarciglia, F., Tiné, V., 2010. Multi-proxy reconstruction of Late Pleistocene to Holocene paleoenvironmental changes in SW Calabria (southern Italy) from marine and continental records. *Il Quaternario – Italian Journal of Quaternary Sciences* 23 (2), 249–256.
- Bernasconi, M.P., Melis, R., Stanley, J.D., 2006. Benthic biofacies to interpret Holocene environmental changes and human impact in Alexandria's Eastern Harbour, Egypt. *The Holocene* 16 (8), 1163–1176.
- Bisculm, M., Colombaroli, D., Vescovi, E., van Leeuwen, J.F.N., Henne, P.D., Rothen, J., Procacci, G., Pasta, S., La Mantia, T., Tinner, W., 2012. Holocene vegetation and fire dynamics in the supra-mediterranean belt of the Nebrodi Mountains (Sicily, Italy). *Journal of Quaternary Science* 27 (7), 687–698.
- Buol, S.W., Hole, F.D., McCracken, R.J., 1989. *Soil Genesis and Classification*, third ed. Iowa State University Press, Ames, p. 446.
- Butzer, K.W., 2005. Environmental history in the Mediterranean world: cross disciplinary investigation of cause-and-effect for degradation and soil erosion. *Journal of Archaeological Science* 32, 1773–1800.
- Caggianelli, A., Prosser, G., Rottura, A., 2000. Thermal history vs. fabric anisotropy in granitoids emplaced at different crustal levels: an example from Calabria, southern Italy. *Terra Nova* 12 (3), 109–116.
- Calanchi, N., De Rosa, R., Mazzuoli, R., Rossi, P.L., Santacroce, R., Ventura, G., 1993. Silicic magma entering a basaltic magma chamber: eruptive dynamics and magma mixing – an example from Salina (Aeolian islands, Southern Tyrrhenian Sea). *Bulletin of Volcanology* 55, 504–522.
- Carcaillet, C., Thimon, M., 1996. Pedoanthracological contribution to the study of the evolution of the upper treeline in the Maurienne Valley (North French Alps): methodology and preliminary data. *Review of Palaeobotany and Palynology* 91, 399–416.
- Catt, J.A., 1989. Relict properties in soils of the central and north-west European temperate region. *Catena Supplement* 16, 41–58.
- Catt, J.A., 1998. Report from working group definitions used in paleopedology. *Quaternary International* 51–52, 84.
- Childs, C.W., Matsue, N., Yoshinaga, N., 1990. Ferrihydrite in volcanic ash soils of Japan. *Soil Science and Plant Nutrition* 37, 299–311.
- Cinque, A., Robustelli, G., Scarciglia, F., Terribile, F., 2000. The dramatic cluster of pyroclastic debris flows which occurred on 5th and 6th May 1998 on the Sarno

- Mountains (Vesuvius region, Southern Italy): a geomorphological perspective. In: Bromhead, E., Dixon, N., Ibsen, M.-L. (Eds.), *Landslides in Research, Theory and Practice*, 1. Thomas Telford Ltd, London, pp. 273–278.
- Colombaroli, D., Marchetto, A., Tinner, W., 2007. Long-term interactions between Mediterranean climate, vegetation and fire regime at Lago di Massaciuccoli (Tuscany, Italy). *Journal of Ecology* 95, 755–770.
- Colombo, C., Sellitto, M.V., Palumbo, G., Terribile, F., Stoops, G., 2007. Characteristics and genesis of volcanic soils from south central Italy: Mt. Gauro (Phlegrean Fields, Campania) and Vico Lake (Latium). In: Arnalds, Ó., Bartoli, F., Buurman, P., Óskarsson, H., Stoops, G., García-Rodeja, E. (Eds.), *Soils of Volcanic Regions in Europe*. Springer, Berlin, pp. 197–229.
- Colacino, M., Conte, M., Piervitali, E., 1997. Elementi di climatologia della Calabria. In: Guerrini, A. (Ed.), *Collana Progetto Strategico "Clima, ambiente e territorio nel Mezzogiorno"*. CNR-IFA (Istituto di Fisica dell'Atmosfera), Roma, p. 218.
- Costantini, E.A.C., 1993. Surface morphology and thinning grade effect on soils of a Calabrian Pine plantation in the Sila Mountain (Calabria Italy). *Geografia Fisica e Dinamica Quaternaria* 16, 29–35.
- Costantini, E.A.C., Priori, S., Urban, B., Hilgers, A., Sauer, D., Protano, G., Trombino, L., Hülle, D., Nannoni, F., 2009. Multidisciplinary characterization of the middle Holocene eolian deposits of the Elsa River basin (central Italy). *Quaternary International* 209, 107–130.
- Crevaschi, M., Trombino, L., 1998. The palaeoclimatic significance of paleosols in Southern Fezzan (Libyan Sahara): morphological and micromorphological aspects. *Catena* 34, 131–156.
- Crisci, G.M., De Rosa, R., Esperanca, S., Mazzuoli, R., Sonnino, M., 1991. Temporal evolution of a three component system: the Island of Lipari (Aeolian Arc, southern Italy). *Bulletin of Volcanology* 53, 207–221.
- Critelli, S., 1999. The interplay of lithospheric flexure and thrust accommodation in forming stratigraphic sequences in the southern Apennines foreland basin system, Italy. *Accademia Nazionale dei Lincei, Rendiconti Lincei Scienze Fisiche e Naturali* 10, 257–326.
- Dahlgren, R., Shoji, S., Nanzyo, M., 1993. Mineralogical characteristics of volcanic ash soils. In: Shoji, S., Nanzyo, M., Dahlgren, R. (Eds.), *Volcanic Ash Soil. Genesis, Properties and Utilization*. Development in Soil Science, vol. 21. Elsevier, Amsterdam, pp. 101–143.
- deMenocal, P.B., 2001. Cultural response to climate change during the Late Holocene. *Science* 292, 667–673.
- De Rosa, R., Guillo, H., Mazzuoli, R., Ventura, G., 2003. New unspiked K–Ar ages of volcanic rocks of the central and western sector of the Aeolian Islands: reconstruction of the volcanic stages. *Journal of Volcanology and Geothermal Research* 120, 161–178.
- Di Donato, V., Esposito, P., Russo Ermolli, E., Cheddadi, R., Scarano, A., 2008. Coupled atmospheric and marine palaeoclimatic reconstruction for the last 35 kyr in the Sele Plain-Gulf of Salerno area (southern Italy). *Quaternary International* 190, 146–157.
- Dimase, A.C., Bonazzi, A., Iovino, F., 1996. Effetti dell'impatto antropico sull'erosione dei suoli dell'altopiano della Sila (Calabria). *Annali dell'Accademia Italiana di Scienze Forestali XLV*, 1–23.
- Di Pasquale, G., Marziano, M., Impagliazzo, S., Lubritto, C., De Natale, A., Bader, M.Y., 2008. The Holocene treeline in the northern Andes (Ecuador): first evidence from soil charcoal. *Palaeogeography, Palaeoclimatology, Palaeoecology* 259 (1), 17–34.
- Di Rita, F., Magri, D., 2009. Holocene drought, deforestation and evergreen vegetation development in the central Mediterranean: a 5500 year record from Lago Alimini Piccolo, Apulia, southeast Italy. *The Holocene* 19 (2), 295–306.
- Dramis, F., Umer, M., Calderoni, G., Haile, M., 2003. Holocene climate phases from buried soils in Tigray (northern Ethiopia): comparison with lake level fluctuations in the Main Ethiopian Rift. *Quaternary Research* 60, 274–283.
- Drysdale, R.N., Zanchetta, G., Hellstrom, J., Maas, R., Fallick, A., Pickett, M., Cartwright, I., Piccini, L., 2006. Late Holocene drought responsible for the collapse of Old World civilization is recorded in an Italian cave flowstone. *Geology* 34, 101–104.
- Dubroeuq, D., Geissert, D., Quantin, P., 1998. Weathering and soil forming processes under semi-arid conditions in two Mexican volcanic ash soils. *Geoderma* 86, 99–122.
- Duchaufour, P., 1982. *Pedology*. George Allen and Unwin, London, p. 448.
- Egli, M., Mastrodonato, G., Seiler, R., Raimondi, S., Favilli, F., Crimi, V., Krebs, R., Cherubini, P., Certini, G., 2012. Charcoal and stable soil organic matter as indicators of fire frequency, climate and past vegetation in volcanic soils of Mt. Etna, Sicily. *Catena* 88, 14–26.
- Egli, M., Nater, M., Mirabella, A., Raimondi, S., Plötze, M., Alioth, L., 2008. Clay minerals, oxyhydroxide formation, element leaching and humus development in volcanic soils. *Geoderma* 143, 101–114.
- Favilli, F., Cherubini, P., Collenberg, M., Egli, M., Sartori, G., Schoch, W., Haerberli, W., 2010. Charcoal fragments of Alpine soils as an indicator of landscape evolution during the Holocene in Val di Sole (Trentino, Italy). *The Holocene* 20 (1), 67–79.
- Fieldes, M., Perrott, K.W., 1966. The nature of allophane in soils: 3. Rapid field and laboratory test for allophane. *New Zealand Journal of Science* 9, 623–629.
- Figueiral, I., Mosbrugger, V., 2000. A review of charcoal analysis as a tool for assessing Quaternary and Tertiary environments: achievements and limits. *Palaeogeography, Palaeoecology, Palaeoclimatology* 164, 397–407.
- FitzPatrick, E.A., 1984. *Micromorphology of Soils*. Chapman & Hall, London, p. 433.
- Frezzotti, M., Narcisi, B., 1996. Late Quaternary tephra-derived paleosols in central Italy's carbonate Apennine Range: stratigraphical and paleoclimatological implications. *Quaternary International* 34–36, 147–153.
- García-Rodeja, E., Nóvoa, J.C., Pontevedra, X., Martínez-Cortizas, A., Buurman, P., 2007. Aluminium and iron fractionation of European volcanic soils by selective dissolution techniques. In: Arnalds, Ó., Bartoli, F., Buurman, P., Óskarsson, H., Stoops, G., García-Rodeja, E. (Eds.), *Soils of Volcanic Regions in Europe*. Springer, Berlin, pp. 325–351.
- Gérard, M., Caquineau, S., Pinheiro, J., Stoops, G., 2007. Weathering and allophane neoformation in soils developed on volcanic ash in the Azores. *European Journal of Soil Science* 58, 496–515.
- Giraudi, C., 2007. Le variazioni climatiche in Italia Centrale negli ultimi 10.000 anni. In: Wezel, F. (Ed.), 2007. Variabilità naturale del clima nell'Olocene ed in tempi storici: un approccio geologico, 1. Quaderni della Società Geologica, pp. 18–24.
- Giraudi, C., Magny, M., Zanchetta, G., Drysdale, R.N., 2011. The Holocene climatic evolution of Mediterranean Italy: a review of the continental geological data. *The Holocene* 21 (1), 105–115.
- Gregory, K.J., Benito, G., Dikau, R., Golosov, V., Jones, A.J.J., Macklin, M.G., Parsons, A.J., Passmore, D.G., Poesen, J., Starkel, L., Walling, D.E., 2006. Past hydrological events related to understanding global change: an ICSU research project. *Catena* 66, 2–13.
- Greguss, P., 1955. Identification of Living Gymnosperms on the Basis of Xylotomy. *Akadémiai Kiadó, Budapest*, p. 263.
- Greguss, P., 1959. *Holz Anatomie der Europäischen Laubbölzer und Sträucher*. Akadémiai Kiadó, Budapest, p. 330.
- Hughes, R.E., Moore, D.M., Glass, H.D., 1994. Qualitative and quantitative analysis of clay minerals in soils. In: Luxmoore, R.J., Amonette, J.E., Zelazny, L.W., Bartels, J.M. (Eds.), *Quantitative Methods in Soil Mineralogy*. Soil Science Society of America. Miscellaneous Publication, Madison, WI, pp. 330–359.
- Huisman, D.J., Jongmans, A.G., Raemaekers, D.C.M., 2009. Investigating Neolithic land use in Swifterbant (NL) using micromorphological techniques. *Catena* 78, 185–197.
- Hunt, C.O., Elrishi, H.A., Gilbertson, D.D., Grattan, J., McLaren, S., Pyatt, F.B., Rushworth, G., Barker, G.W., 2004. Early-holocene environments in the Wadi Faynan, Jordan. *The Holocene* 14 (6), 921–930.
- Huntley, B., Watts, W.A., Allen, J.R.M., Zolitschka, B., 1999. Palaeoclimate, chronology and vegetation history of the Weichselian Lateglacial: comparative analysis of data from three cores at Lago Grande di Monticchio, southern Italy. *Quaternary Science Reviews* 18, 945–960.
- ICOMAND, 1988. Circular Letter No. 10. International Committee on the Classification of Andisols. New Zealand Soil Bureau, Lower Hutt, New Zealand.
- IUSS Working Group WRB, 2007. World Reference Base for Soil Resources 2006 – a Framework for International Classification, Correlation and Communication. First update 2007. World Soil Resources Reports No. 103. FAO, Rome, p. 116.
- Jalut, G., Dedoubat, J.J., Fontugne, M., Otto, T., 2009. Holocene circum-Mediterranean vegetation changes: climate forcing and human impact. *Quaternary International* 200, 4–18.
- James, P., Chester, D., Duncan, A., 2000. Volcanic Soils: Their Nature and Significance for Archaeology. In: Geological Society of London, Special Publication 171, pp. 317–338.
- Joannin, S., Brugiapaglia, E., De Bealieu, J.L., Bernardo, L., Magny, M., Peyron, O., Goring, S., Vannière, B., 2012. Pollen-based reconstruction of Holocene vegetation and climate in southern Italy: the case of Lago Trifoglietti. *Climate of the Past* 8, 1973–1996.
- Jongerijs, A., 1970. Some morphological aspects of regrouping phenomena in Dutch soils. *Geoderma* 4, 311–331.
- Keller, J., 1980. The Island of Salina. In: *Rendiconti della Società Italiana di Mineralogia e Petrologia*, vol. 36, pp. 489–524.
- Kemp, R.A., 1998. Role of micromorphology in paleopedological research. *Quaternary International* 51–52, 133–141.
- Köppen, W., 1936. *Das geographische system der klimate*. In: Köppen, W., Geiger, R. (Eds.), *Handbuch der Klimatologie* 1, Part C. Gebruder Borntraeger, Berlin, p. 46.
- Kretzschmar, R., Robarge, W.P., Amoozegar, A., Vepraskas, M.J., 1997. Biotite alteration to halloysite and kaolinite in soil-saprolite profiles developed from mica schist and granite gneiss. *Geoderma* 75, 155–170.
- Kühn, P., Aguilar, J., Miedema, R., 2010. Textural features and related horizons. In: Stoops, G., Marcelino, V., Mees, F. (Eds.), *Interpretation of Micromorphological Features of Soils and Regoliths*. Elsevier, Amsterdam, pp. 217–250.
- Liotta, D., Caggianelli, A., Kruhl, J.H., Festa, V., Prosser, G., Langone, A., 2008. Multiple injections of magmas along a Hercynian mid-crustal shear zone (Sila Massif, Calabria, Italy). *Journal of Structural Geology* 30, 1202–1217.
- Linstädter, A., Zielhofer, C., 2010. Regional fire history shows abrupt responses of Mediterranean ecosystems to centennial-scale climate change (Olea-Pistacia woodlands, NE Morocco). *Journal of Arid Environments* 74, 101–110.
- Madella, M., Fuller, D.Q., 2006. Palaeoecology and the Harappan Civilisation of South Asia: a reconsideration. *Quaternary Science Reviews* 25, 1283–1301.
- Magny, M., Joannin, S., Galop, D., Vannière, B., Haas, J.N., Bassetti, M., Bellintani, P., Scandolari, R., Desmet, M., 2012a. Holocene palaeohydrological changes in the northern Mediterranean borderlands as reflected by the lake-level record of Lake Ledro, northeastern Italy. *Quaternary Research* 77, 382–396.
- Magny, M., Peyron, O., Sadori, L., Ortu, E., Zanchetta, G., Vannière, B., Tinner, W., 2012b. Contrasting patterns of precipitation seasonality during the Holocene in the south- and north-central Mediterranean. *Journal of Quaternary Science* 27 (3), 290–296.

- Marchetto, A., Colombaroli, D., Tinner, W., 2008. Diatom response to mid-Holocene climate change in Lago di Massaciuccoli (Tuscany, Italy). *Journal of Paleolimnology* 40, 235–245.
- Marino, D., Talianno Grasso, A., 2008. Dai primi uomini al tardo impero nel cuore della Calabria. In: Sila, Magna (Ed.), *Ricerche archeologiche e storiche in Calabria: Modelli e prospettive*. Conference proceedings, Istituto per gli Studi Storici di Cosenza, 24 March 2007, Editoriale Progetto 2000, Cosenza, Italy, pp. 65–92.
- Marino, D., Talianno Grasso, A., 2010. Ricerche topografiche e scavi archeologici nella Sila Grande. In: *Atlante Tematico di Topografia Antica – ATTA 20*. «L'Erma» di Bretschneider, Roma, pp. 51–78.
- Meijer, E.L., Buurman, P., Fraser, A., García-Rodeja, E., 2007. Extractability and FTIR-characteristics of poorly-ordered minerals in a collection of volcanic ash soils. In: Arnalds, Ó., Bartoli, F., Buurman, P., Óskarsson, H., Stoops, G., García-Rodeja, E. (Eds.), *Soils of Volcanic Regions in Europe*. Springer, Berlin, pp. 155–180.
- Mercuri, A.M., Sadori, L., Uzquiano Ollero, O., 2011. Mediterranean and north-African cultural adaptations to mid-Holocene environmental and climatic changes. *The Holocene* 21 (1), 189–206.
- Messina, A., Compagnoni, R., De Vivo, B., Perrone, V., Russo, S., Barbieri, M., Scott, B., 1991. Geological and petrochemical study of the Sila Massif plutonic rocks (northern Calabria, Italy). *Bollettino della Società Geologica Italiana* 110, 165–206.
- Migowski, C., Stein, M., Prasad, S., Negendank, J.F.W., Agnong, A., 2006. Holocene climate variability and cultural evolution in the Near East from the Dead Sea sedimentary record. *Quaternary Research* 66, 421–431.
- MiPAF (Ministero delle Politiche Agricole e Forestali), 2000. Osservatorio Nazionale Pedologico e per la Qualità del Suolo. International Society of Soil Science, Società Italiana della Scienza del Suolo. Metodi di analisi chimica del suolo. Franco Angeli Editore, Milano, Italy. fascicolated.
- Mizota, C., van Reeuwijk, L.P., 1989. Clay Mineralogy and Chemistry of Soils Formed in Volcanic Material in Diverse Climatic Regions. International Soil Reference and Information Centre Soil Monograph 2. ISRIC, Wageningen, p. 185.
- Molin, P., Pazzaglia, F.J., Dramis, F., 2004. Geomorphic expression of active tectonics in a rapidly-deforming forearc, Sila Massif, Calabria, Southern Italy. *American Journal of Science* 304, 559–589.
- Montgomery, D.R., 2007. *Dirt: The Erosion of Civilizations*. University of California Press, Berkeley, p. 294.
- Moore, D.M., Reynolds Jr., R.C., 1997. *X-ray Diffraction and the Identification and Analysis of Clay Minerals*, second ed. Oxford University Press, Oxford, UK, p. 378.
- Nanzoy, M., Dahlgren, R., Shoji, S., 1993. Chemical characteristics of volcanic ash soils. In: Shoji, S., Nanzoy, M., Dahlgren, R. (Eds.), *Volcanic Ash Soil. Genesis, Properties and Utilization*. Development in Soil Science, 21. Elsevier, Amsterdam, pp. 145–187.
- Overpeck, J., Whitlock, C., Huntley, B., 2003. Terrestrial biosphere dynamics in the climate system: past and future. In: Alverson, K.D., Bradley, R.S., Pedersen, T.F. (Eds.), *Paleoclimate, Global Change, and the Future*. Springer-Verlag, Berlin Heidelberg, pp. 81–104.
- Pang, J., Hu, X., Huang, C., Zhang, X., 2006. Micromorphological features of old cultivated and modern soils in Guanzhong areas, Shaanxi Province, China. *Agricultural Sciences in China* 5 (9), 691–699.
- Parfitt, R.L., 2009. Allophane and imogolite: role in soil biogeochemical processes. *George Brown Lecture 2008*. *Clay Minerals* 44, 135–155.
- Parfitt, R.L., Henmi, T., 1982. Comparison of an oxalate extraction method and infrared spectroscopic method for determining allophane in soil clays. *Soil Science and Plant Nutrition* 28, 183–190.
- Parfitt, R.L., Saigusa, M., Cowie, J.D., 1984. Allophane and halloysite formations in a volcanic ash bed under different moisture conditions. *Soil Science* 138, 360–364.
- Parfitt, R.L., Kimble, J.M., 1989. Conditions for formation of allophane in soils. *Soil Science Society of America Journal* 53, 971–977.
- Parfitt, R.L., Wilson, A.D., 1985. Estimation of allophane and halloysite in three sequences of volcanic soils, New Zealand. In: Fernandez Caldas, E., Yaalon, D.H. (Eds.), *Volcanic Soils*. Catena Supplement 7. Braunschweig. Catena Verlag, Desdedt, Germany, pp. 1–8.
- Pelle, T., Scarciglia, F., Allevato, E., Di Pasquale, G., La Russa, M.F., Marino, D., Natali, E., Robustelli, G., Tiné, V., 2013. Reconstruction of Holocene environmental changes in two archaeological sites of Calabria (Southern Italy) using an integrated pedological and anthracological approach. *Quaternary International* 288, 206–214.
- Peyron, O., Goring, S., Dormoy, I., Kothhoff, U., Pross, J., de Beaulieu, J.-L., Drescher-Schneider, R., Vannié, B., Magny, M., 2011. Holocene seasonality changes in the central Mediterranean region reconstructed from the pollen sequences of Lake Acesa (Italy) and Tenaghi Philippon (Greece). *The Holocene* 21 (1), 131–146.
- Piccarreta, M., Caldara, M., Capolongo, D., Boenzi, F., 2011. Holocene geomorphic activity related to climatic change and human impact in Basilicata, Southern Italy. *Geomorphology* 128 (3–4), 137–147.
- Pignatti, S., 1982. *Flora d'Italia*. Edagricole, Bologna, 3 issues.
- Quézel, P., Médail, F., 2003. *Ecologie et biogéographie des forêts du Bassin Méditerranéen*. Elsevier, Collection Environnement, Paris, 573.
- Roberts, N., Brayshaw, D., Kuzucuoglu, C., Perez, R., Sadori, L., 2011. The mid-Holocene climatic transition in the Mediterranean: causes and consequences. *The Holocene* 21 (1), 3–13.
- Roberts, N., Reed, J.M., Leng, M.J., Kuzucuoglu, C., Fontugne, M., Bertaux, J., Woldring, H., Bottema, S., Black, S., Hunt, E., Karabiyikoglu, M., 2001. The tempo of Holocene climatic change in the eastern Mediterranean region: new high-resolution crater-lake sediment data from central Turkey. *The Holocene* 11 (6), 721–736.
- Roberts, N., Stevenson, A.C., Davis, B., Cheddadi, R., Brewer, S., Rosen, A., 2004. Holocene climate, environment and cultural change in the circum-Mediterranean region. In: Battarbee, R.W., Gasse, F., Stickley, C. (Eds.), *Past Climate Variability Through Europe and Africa*. Springer, Dordrecht, pp. 343–362.
- Roda, C., 1964. Distribuzione e facies dei sedimenti neogenici nel Bacino Crotonese. *Geologica Romana* 3, 319–366.
- Rossignol-Strick, M., 1999. The Holocene climatic optimum and pollen records of sapropel 1 in the eastern Mediterranean, 9000–6000 BP. *Quaternary Science Reviews* 18, 515–530.
- Sadori, L., Giraudi, C., Petitti, P., Ramrath, A., 2004. Human impact at Lago di Mezzano (central Italy) during the Bronze Age: a multidisciplinary approach. *Quaternary International* 113, 5–17.
- Sadori, L., Narcisi, B., 2001. The Postglacial record of environmental history from Lago di Pergusa, Sicily. *The Holocene* 11 (6), 655–670.
- Sadori, L., Zanchetta, G., Giardini, M., 2008. Last Glacial to Holocene palaeoenvironmental evolution at Lago di Pergusa (Sicily, Southern Italy) as inferred by pollen, microcharcoal, and stable isotopes. *Quaternary International* 181, 4–14.
- Sauro, U., Borsato, A., Frisia, S., Madonia, G., Piccini, L., Tuccimei, P., Camuffo, D., Cucchi, F., Forti, P., Macaluso, T., Miorandi, R., Paladini, M., Salzano, R., Shopov, Y., Spötl, C., Stoykova, D., Zini, L., 2003. Variabilità climatica nel Tardiglaciale e nell'Olocene da dati di speleotemi lungo una traversa N-S in Italia. *Studi Trentini di Scienze Naturali. Acta Geologica* 80, 175–184.
- Scarciglia, F., Le Pera, E., Critelli, S., 2005a. Weathering and pedogenesis in the Sila Grande Massif (Calabria, South Italy): from field scale to micromorphology. *Catena* 61 (1), 1–29.
- Scarciglia, F., Le Pera, E., Vecchio, G., Critelli, S., 2005b. The interplay of geomorphic processes and soil development in an upland environment, Calabria, South Italy. *Geomorphology* 69 (1–4), 169–190.
- Scarciglia, F., Le Pera, E., Critelli, S., 2007. The onset of the sedimentary cycle in a mid-latitude upland environment: weathering, pedogenesis, and geomorphic processes on plutonic rocks (Sila Massif, Calabria). In: Arribas, J., Critelli, S., Johnsson, M.J. (Eds.), *Sedimentary Provenance and Petrogenesis: Perspectives from Petrography and Geochemistry*. Geological Society of America Special Paper 420, pp. 149–166.
- Scarciglia, F., De Rosa, R., Vecchio, G., Apollaro, C., Robustelli, G., Terrasi, F., 2008. Volcanic soil formation in Calabria (southern Italy): the Cecita Lake geosol in the late Quaternary geomorphological evolution of the Sila uplands. *Journal of Volcanology and Geothermal Research* 177 (1), 101–117.
- Scarciglia, F., Robustelli, G., Tiné, V., La Russa, M.F., Abate, M., Pezzino, A., 2009. The role of human impacts and Holocene climate change in the Santuario della Madonna Cave (Calabria). In: Amato, V., Marriner, N., Morhange, C., Romano, P., Russo Ermolli, E. (Eds.), *Geoarcheology in Italy, Méditerranée* 112, pp. 137–143.
- Schweingruber, F.H., 1990. *Anatomy of European Woods*. Stuttgart. Paul Haupt Berne and Stuttgart Publishers, Berne, p. 800.
- Schwertmann, U., 1964. Differenzierung der Eisenoxyde des Bodens durch photochemische Extraktion mit saurer Ammoniumoxalat-Lösung. *Zeitschrift für Pflanzenernährung, Düngung und Bodenkunde* 105, 194–202.
- Sequeira Braga, M.A., Paquet, H., Begonia, A., 2002. Weathering of granites in a temperate climate (NW Portugal): granitic saprolites and arenization. *Catena* 49, 41–56.
- Shoji, S., Dahlgren, R., Nanzoy, M., 1993. Genesis of volcanic ashsoils. In: Shoji, S., Nanzoy, M., Dahlgren, R. (Eds.), *Volcanic Ash Soils: Genesis, Properties and Utilization*. Elsevier, Amsterdam, pp. 37–71.
- Soil Survey Staff, 2010. *Keys to Soil Taxonomy*, eleventh ed. United States Department of Agriculture (USDA) – Natural Resources Conservation Service (NRCS), Washington DC, p. 338.
- Sorriso-Valvo, M., 1993. The geomorphology of Calabria. A sketch. *Geografia Fisica e Dinamica Quaternaria* 16, 75–80.
- Taboada, T., García, C., 1999. Pseudomorphic transformation of plagioclases during the weathering of granitic rocks in Galicia (NW Spain). *Catena* 35, 291–302.
- Tanguy, J.-C., Le Goff, M., Principe, C., Arrighi, S., Chillemi, V., Paiotti, A., La Delfa, S., Patanè, G., 2003. Archeomagnetic dating of Mediterranean volcanics of the last 2100 years: validity and limits. *Earth and Planetary Science Letters* 211, 111–124.
- Terribile, F., Basile, A., De Mascellis, R., Iamarino, M., Magliulo, P., Pepe, S., Vingiani, S., 2007. Landslide processes and Andosols: the case study of the Campania region, Italy. In: Arnalds, Ó., Bartoli, F., Buurman, P., Óskarsson, H., Stoops, G., García-Rodeja, E. (Eds.), *Soils of Volcanic Regions in Europe*. Springer, Berlin, pp. 545–563.
- Thornycraft, V.R., Benito, G., 2006. Late Holocene fluvial chronology of Spain: the role of climatic variability and human impact. *Catena* 66, 34–41.
- Tinner, W., van Leeuwen, J.F.N., Colombaroli, D., Vescovi, E., van der Knaap, W.O., Henne, P.D., Pasta, S., D'Angelo, S., LaMantia, T., 2009. Holocene environmental and climatic changes at Gorgo Basso, a coastal lake in southern Sicily, Italy. *Quaternary Science Reviews* 28, 1498–1510.
- Touflan, P., Talon, B., 2009. Spatial reliability of soil charcoal analysis: the case of subalpine forest soils. *Ecoscience* 6, 23–27.

- Touflan, P., Talon, B., Walsh, K., 2010. Soil charcoal analysis: a reliable tool for spatially precise studies of past forest dynamics: a case study in the French Southern Alps. *The Holocene* 20 (1), 45–52.
- Tranne, C.A., Lucchi, F., Calanchi, N., Lanzafame, G., Rossi, P.L., 2002. Geological Map of the Island of Lipari (Aeolian Islands). LAC – Litografia Artistica Cartografica, Firenze, Italy.
- Turney, C.S.M., Brown, H., 2007. Catastrophic early Holocene sea level rise, human migration and the Neolithic transition in Europe. *Quaternary Science Reviews* 26, 2036–2041.
- Tursina, T.V., 2009. Methodology for the diagnostics of soil polygenesis on the basis of macro- and micromorphological studies. *Journal of Mountain Science* 6, 125–131.
- Usai, M.R., 2001. Textural pedofeatures and pre-Hadrian's wall ploughed paleosols at Stanwix, Carlisle, Cumbria, U.K. *Journal of Archaeological Science* 28, 541–553.
- Vacca, A., Adamo, P., Pigna, M., Violante, P., 2003. Genesis of tephra-derived soils from the Roccamonfina Volcano, South Central Italy. *Soil Science Society of America Journal* 67, 198–207.
- Van Dijk, J.P., Bello, M., Brancaleoni, G.P., Cantarella, G., Costa, V., Frixa, A., Golfetto, F., Merlini, S., Riva, M., Torricelli, S., Toscano, C., Zerilli, A., 2000. A regional structural model for the northern sector of the Calabrian Arc (southern Italy). *Tectonophysics* 324, 267–320.
- van der Marel, H.W., Krohmer, P., 1969. O-H stretching vibrations in kaolinite, and related minerals. *Contributions to Mineralogy and Petrology* 22, 73–82.
- Vanniere, B., Power, M.J., Roberts, N., Tinner, W., Carrión, J., Magny, M., Bartlein, P., Colombaroli, D., Daniau, A.L., Finsinger, W., Gil-Romera, G., Kaltenrieder, P., Pini, R., Sadori, L., Turner, R., Valsecchi, V., Vescovi, E., 2011. Circum-Mediterranean fire activity and climate changes during the mid-Holocene environmental transition (8500–2500 cal. BP). *The Holocene* 21, 53–73.
- Versace, P., Ferrari, E., Gabriele, S., Rossi, F., 1989. Valutazione delle piene in Calabria. In: CNR-IRPI (Istituto di Ricerca per la Protezione Idrogeologica), *Geodata* 30, p. 232.
- Warner, K., Hamza, M., Oliver-Smith, A., Renaud, F., Julca, A., 2010. Climate change, environmental degradation and migration. *Natural Hazards* 55, 689–715.
- Wilson, C., Simpson, I.A., Currie, E.J., 2002. Soil management in pre-Hispanic raised field systems: micromorphological evidence from Hacienda Zuleta, Ecuador. *Geoarchaeology* 17 (3), 261–283.
- Wilson, M.J. (Ed.), 1987. *A Handbook of Determinative Methods in Clay Mineralogy*. Blackie and Sons, Glasgow, p. 308.
- Zanchetta, G., Sulpizio, R., Roberts, N., Cioni, R., Eastwood, W.J., Siani, G., Caron, B., Paterne, M., Santacrose, R., 2011. Tephrostratigraphy, chronology and climatic events of the Mediterranean basin during the Holocene: an overview. *The Holocene* 21 (19), 33–52.
- Zanchetta, G., Van Welden, A., Baneschi, I., Drysdale, R., Sadori, L., Roberts, N., Giardini, M., Beck, C., Pascucci, V., Sulpizio, R., 2012. Multiproxy record for the last 4500 years from Lake Shkodra (Albania/Montenegro). *Journal of Quaternary Science* 27 (8), 780–789.